JEM Journal of Experimental Medicine

ARTICLE

Overexpression of *Lmo2* initiates T-lymphoblastic leukemia via impaired thymocyte competition

Hesham D. Abdulla[1,2], Raed Alserihi[1,2,3], Christoffer Flensburg[1,2], Waruni Abeysekera[1,2], Meng-Xiao Luo[1,2], Daniel H.D. Gray[1,2], Xiaodong Liu[4,5,6], Gordon K. Smyth[1,7], Warren S. Alexander[1,2], Ian J. Majewski[1,2], and Matthew P. McCormack[1,2,8,9]

Cell competition has recently emerged as an important tumor suppressor mechanism in the thymus that inhibits autonomous thymic maintenance. Here, we show that the oncogenic transcription factor *Lmo2* causes autonomous thymic maintenance in transgenic mice by inhibiting early T cell differentiation. This autonomous thymic maintenance results in the development of self-renewing preleukemic stem cells (pre-LSCs) and subsequent leukemogenesis, both of which are profoundly inhibited by restoration of thymic competition or expression of the antiapoptotic factor BCL2. Genomic analyses revealed the presence of *Notch1* mutations in pre-LSCs before subsequent loss of tumor suppressors promotes the transition to overt leukemogenesis. These studies demonstrate a critical role for impaired cell competition in the development of pre-LSCs in a transgenic mouse model of T cell acute lymphoblastic leukemia (T-ALL), implying that this process plays a role in the ontogeny of human T-ALL.

Introduction

T cell acute lymphoblastic leukemia (T-ALL) is an acute, predominantly pediatric cancer caused by the multistep transformation of developing T cell progenitors in the thymus (Belver and Ferrando, 2016; Girardi et al., 2017; Iacobucci and Mullighan, 2017). A hallmark of T-ALL is overexpression of oncogenic transcription factors, with most cases containing chromosomal abnormalities that cause overexpression of transcription factors that are normally silenced during early stages of T cell development. Commonly targeted transcription factors include basic helix-loop-helix factors (TAL1, LYL1, and TAL2) and their binding partners, the Lim-domain only proteins, LMO1 or LMO2, as well as homeobox transcription factors including the HOXA cluster, TLX1, and TLX3. These transcription factors are complemented by additional mutations that commonly affect NOTCH and JAK/STAT signaling, tumor suppressors, protein translation, and epigenetic pathways (Belver and Ferrando, 2016; Girardi et al., 2017; Iacobucci and Mullighan, 2017). However, the molecular and cellular effects of oncogenic transcription factors on T cell development, as well as how they interact with secondary mutations to cause T-ALL, remain poorly understood.

LMO2 is an oncogenic transcription factor that is overexpressed in up to half of all T-ALL cases (Ferrando et al., 2002; Wu et al., 2015) due to chromosomal translocations, loss of insulator boundaries, or non-coding mutations that result in neomorphic promoters (Abraham et al., 2017; Chen et al., 2011; Dik et al., 2007; Goossens and Van Vlierberghe, 2017; Hnisz et al., 2016; Rahman et al., 2017; Van Vlierberghe et al., 2006; Wu et al., 2015). In addition, *LMO2* was targeted by retroviral insertion mutagenesis in four out of five cases of T-ALL that arose during gene therapy trials for X-linked severe combined immunodeficiency (X-SCID; Hacein-Bey-Abina et al., 2008; Hacein-Bey-Abina et al., 2003; Howe et al., 2008; McCormack and Rabbitts, 2004) as well as in six cases of T-ALL that occurred following similar gene therapy for Wiskott–Aldrich Syndrome (Braun et al., 2014). *LMO2* encodes a small (~20 kD) protein with no DNA binding capacity, which is almost entirely comprised of zinc finger-containing LIM domains that mediate protein–protein interactions. As such, it functions as a bridging molecule that mediates the assembly of multifactorial transcriptional complexes that play critical roles in hematopoietic stem cells (HSCs), erythroid development, and vascular remodeling, as well as aberrant complexes that drive T-ALL development (Chambers and Rabbitts, 2015; Matthews et al., 2013).

To study the role of LMO2 in T-ALL, transgenic mouse models have been developed that recapitulate its overexpression during T cell development in the thymus (Larson et al., 1994; Ruggero et al., 2016; Smith et al., 2014). Using cell lineage tracing

[1]Walter and Eliza Hall Institute of Medical Research, Parkville, Australia; [2]Department of Medical Biology, University of Melbourne, Parkville, Australia; [3]College of Applied Medical Sciences, King Abdul-Aziz University, Jeddah, Saudi Arabia; [4]Westlake Laboratory of Life Sciences and Biomedicine, Hangzhou, China; [5]School of Life Sciences, Westlake University, Hangzhou, China; [6]Westlake Institute for Advanced Study, Hangzhou, China; [7]School of Mathematics and Statistics, University of Melbourne, Parkville, Australia; [8]Australian Centre for Blood Diseases, Monash University, Melbourne, Australia; [9]iCamuno Biotherapeutics, Melbourne, Australia.

Correspondence to Matthew P. McCormack: matthew.mccormack@monash.edu.

in *CD2-Lmo2* transgenic mice, we found that LMO2 induces autonomous thymocyte self-renewal, resulting in a population of transplantable preleukemic stem cells (pre-LSCs) that show serial long-term engraftment capacity and persist for up to 1 yr prior to the development of overt leukemia (McCormack et al., 2010). Subsequent studies have shown that other transcription factors, including the related TAL1 and LMO1 oncoproteins and the fusion protein NUP98-HOXD13, also result in the development of pre-LSCs (Shields et al., 2019; Tremblay et al., 2010). In all three of these models, pre-LSCs share a similar, early T cell precursor (ETP)–like gene expression profile and show an essential requirement for the LMO2 cofactor LYL1, suggesting a common mechanism by which different oncogenic transcription factors cause thymocyte self-renewal (Gerby et al., 2014; Shields et al., 2019). Moreover, recent methylation profiling has provided evidence that most human T-ALL cases derive from self-renewing pre-LSCs (Roels et al., 2020).

Together, the above studies indicate an important role for thymocyte self-renewal in initiating T-ALL. Indeed, thymocytes normally do not self-renew but are maintained by periodic seeding of thymus-settling progenitors (TSPs) from the bone marrow (BM; Boehm, 2012). However, when thymocytes are placed in an environment in which incoming TSPs are defective, for example in mice deficient in the IL-7 receptor common gamma chain, thymus autonomy ensues (Martins et al., 2012; Peaudecerf et al., 2012). In four separate studies (Gao et al., 2019; Ginn et al., 2017; Martins et al., 2014; Schiroli et al., 2017), but not a fifth (Peaudecerf et al., 2016), this situation resulted in T-ALL development, indicating that cell competition is a tumor suppressor mechanism in the thymus. This has prompted speculation that reduced cell competition may have played a role in the development of T-ALL in patients undergoing gene therapy for X-SCID (Ginn et al., 2018; Martins et al., 2014); however, this remains controversial (Peaudecerf et al., 2016; Qasim et al., 2014). Moreover, to date, T-ALL has only been shown in experimental settings of TSP deprivation, and whether cell competition plays a role in oncogene-induced T-ALL is unknown. Here, we investigate this in a model of LMO2-induced T-ALL. We demonstrate that failure of cell competition is critical in the establishment of pre-LSCs and subsequent leukemogenesis. This implies that impaired cell competition is an important mediator of oncogenesis in murine models of T-ALL and may play a key role in human T-ALL pathogenesis.

Results

Neonatal thymi show autonomy when transplanted into *Lmo2*-transgenic mice

We have previously used a cell lineage tracing approach to show that overexpression of *Lmo2* in *CD2-Lmo2* transgenic mice blocks the import of BM-derived progenitors and results in self-renewal of thymocytes from a young age, up to 1 yr prior to the onset of T-ALL (McCormack et al., 2010). To determine whether this property of self-renewal is intrinsic to the thymus, we transplanted thymic lobes from neonatal *Lmo2*-transgenic mice into the kidney capsule of congenic (CD45.1) recipient mice and vice versa. 1 mo later, the percentage of recipient (BM-derived) thymocytes was determined (Fig. 1 A). As expected, WT donor thymi were completely seeded by recipient (BM-derived) cells by 4 wk after transplant (Fig. 1, B and C). Surprisingly, however, *Lmo2*-transgenic neonatal grafts were also completely seeded by recipient-derived cells in WT recipients but were maintained in *Lmo2*-transgenic recipients (Fig. 1, B and C). Furthermore, WT thymi also showed substantial autonomy when engrafted into the kidney capsule of *Lmo2*-transgenic mice, being comprised of mostly donor-derived cells at 4 wk after transplant (Fig. 1, B and C). This suggests a cell non-autonomous effect on thymopoiesis in *Lmo2*-transgenic mice which results in thymic autonomy.

LMO2 blocks T cell development at the DN2 stage

The above results suggested that *CD2-Lmo2* transgenic mice may have a defect in thymic settling progenitors leading to long-term maintenance of downstream T cell progenitors, a situation that has been described previously (Martins et al., 2014; Martins et al., 2012; Peaudecerf et al., 2012). To examine this, we performed competitive BM transplantation using *Lmo2*-transgenic cells (Fig. 2 A). At 4 wk after transplantation, *Lmo2*-transgenic BM gave normal BM engraftment, but strikingly showed an almost complete failure to reconstitute the thymus (Fig. 2, B and C). Analysis of individual progenitor populations showed that *Lmo2*-transgenic progenitors could contribute to BM progenitor populations and early thymocyte stages (ETPs and CD4-CD8 double-negative [DN]2 thymocytes; Fig. 2, D and E). However, there was an almost complete lack of engraftment of *Lmo2*-transgenic cells beyond the DN2 stage (Fig. 2), an effect that persisted at 12 wk after transplant (Fig. 2, D and E). Thus, *Lmo2*-transgenic progenitors can settle the thymus but exhibit a profound developmental block at the DN2 stage of T cell development.

Consistent with a developmental block at the DN2 stage of T cell development, analysis of neonatal (1 wk old) *Lmo2*-transgenic mice showed a clear accumulation of DN2 cells with abnormally high Kit expression that persisted until ∼1 mo of age (Fig. S1, A and B). However, by 2 mo of age, a population of DN3 thymocytes appeared that showed aberrantly high expression of Kit, as previously reported in this model (Larson et al., 1995; McCormack et al., 2010; Fig. S1, A and B). Further analysis showed that these cells were blocked at the DN3a stage, but showed expression of intracellular TCR-β, which is normally expressed from the DN3b stage (Fig. S1, A and C). Analysis of cell cycling status revealed that the accumulating DN2 thymocytes in neonatal *Lmo2*-transgenic mice were highly quiescent (Fig. S1, D and E). While neonatal *Lmo2*-transgenic DN3 thymocytes were also abnormally quiescent, by 2 mo of age, these cells showed normal cycling (Fig. S1, D and E). Thus, *Lmo2* overexpression initially causes a developmental block at the DN2 stage, which is followed by an accumulation of abnormal DN3a thymocytes by 2 mo of age.

Developmentally arrested *Lmo2*-transgenic DN2 thymocytes persist long term but do not expand in vivo

To determine whether *Lmo2* directly enables thymocytes to persist and expand in vivo, *Lmo2*-transgenic lymphoid primed

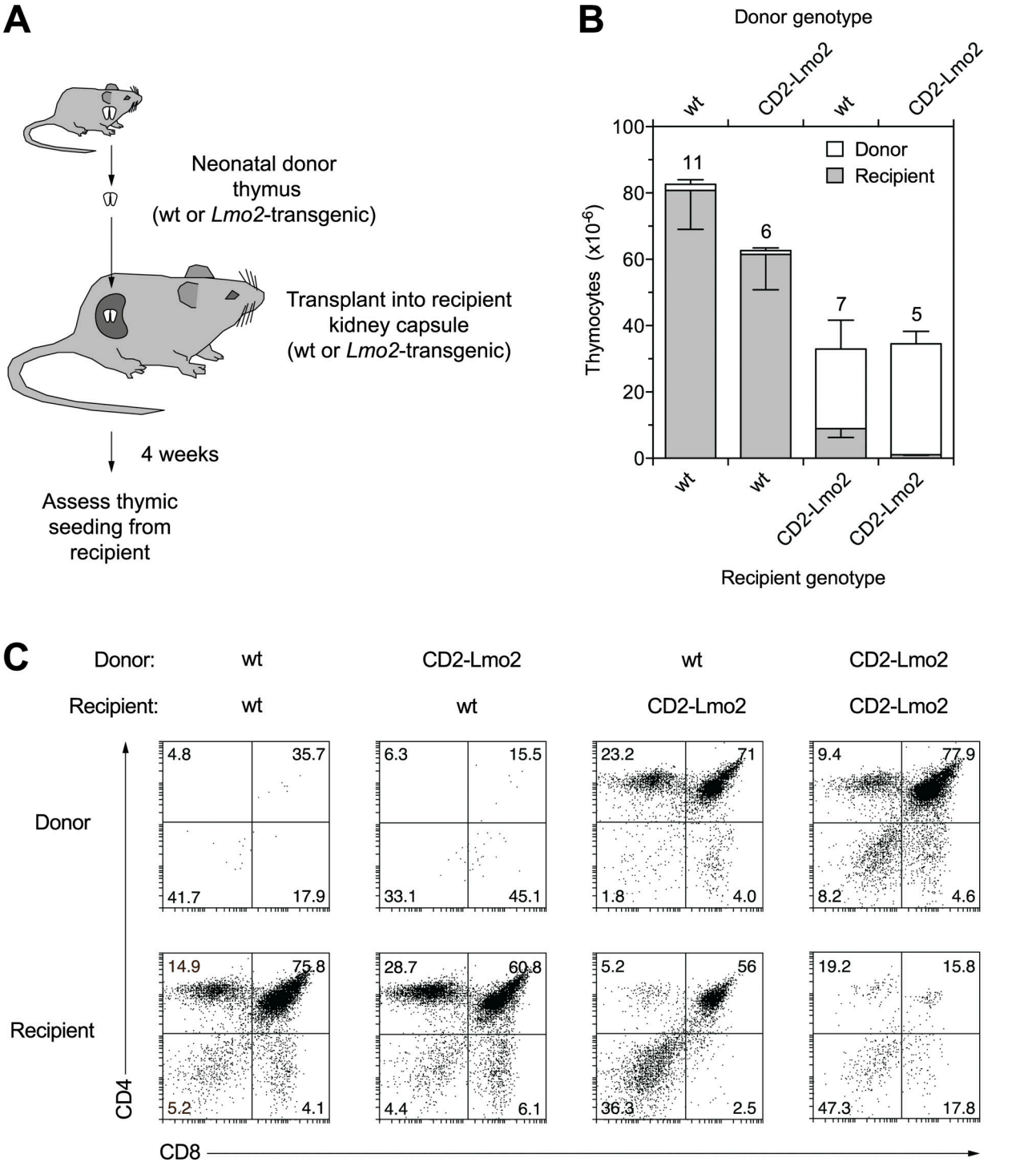

Figure 1. **Cell non-autonomous thymocyte self-renewal in *Lmo2*-transgenic mice. (A)** Schematic of thymic kidney capsule grafting experiment to test autonomy of thymocyte self-renewal in *Lmo2*-transgenic mice. **(B)** Contribution of donor (thymus-derived) vs. recipient (host-derived) cells to grafted thymi at 4 wk after transplant. Bars are mean + SD (donor cells) or – SD (recipient cells), with numbers above the bars indicating the number of replicates. Data are from three separate experiments. **(C)** Representative FACS plots showing the CD4-CD8 profiles of donor (thymus-derived) vs. recipient (host-derived) cells. wt, WT.

multipotent progenitors (LMPPs) were isolated and their potential for long-term thymic engraftment was examined by injecting them directly into the thymi of sublethally irradiated congenic (CD45.1) mice. At 1 mo after transplant, *Lmo2*-transgenic cells showed normal numbers of donor-derived DN2 thymocytes but decreased numbers of downstream thymocyte subsets (Fig. 3, A and B). At 3 mo after transplant, both WT and *Lmo2*-transgenic donor cells showed low levels of donor engraftment (Fig. 3, A and B). However, while the WT donor-derived cells were mostly fully differentiated CD4 T-cells, *Lmo2*-transgenic

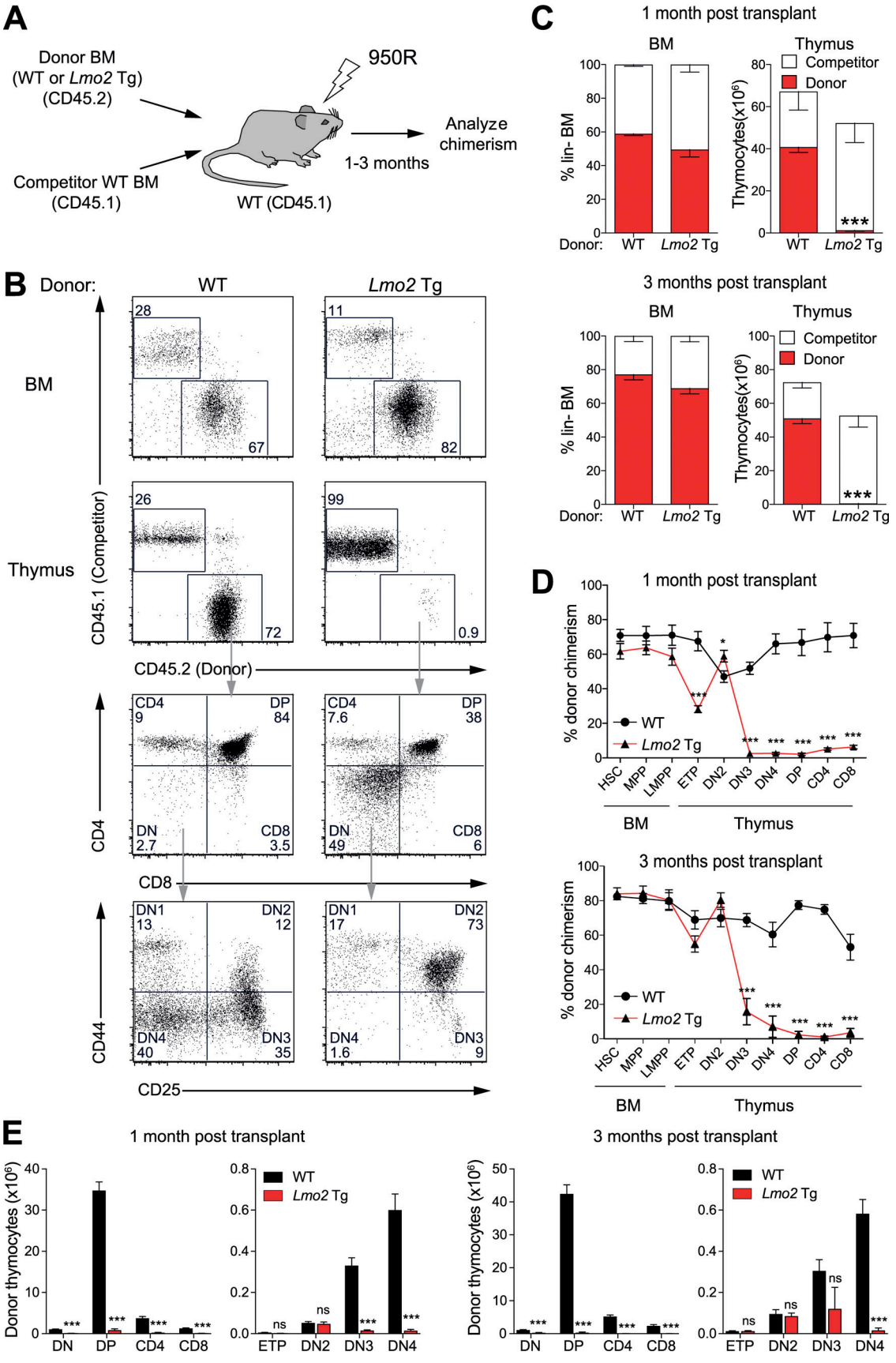

Figure 2. **LMO2 blocks T cell development at the DN2 stage. (A)** Schematic of competitive BM transplantation assay to test contribution of *Lmo2*-transgenic (Tg) BM to T cell development. **(B)** Analysis of donor/competitor contribution to BM and thymus, and phenotypic analysis of donor thymocytes, at

1 mo after transplant. **(C)** Percentage of donor/competitor BM (left panel) and total number of donor/competitor thymocytes (right panel) at 1 and 3 mo after transplant. Results are mean – SEM (top panels). **(D)** Contribution of donor BM of the indicated genotypes to progenitor populations in the BM (HSC, multipotent progenitor [MPP], and LMPP) and stages of T cell development in the thymus (ETP, DN2, DN3, DN4, CD4-CD8 DP, CD4, and CD8) at 1 and 3 mo after transplant. Results are mean ± SEM. **(E)** Absolute numbers of donor T cell subsets at 1 and 3 months after transplant. Results are mean + SEM. Data are from n = 8–12 total recipients from three to four donor mice from two independent experiments. *P < 0.05, ***P < 0.001 vs. WT (Student's T test).

LMPP-derived cells still contained significant numbers of donor-derived DN2 thymocytes, with an average of 6,500 DN2 cells remaining (Fig. 3, A and B). As this was ∼10% of the number of donor-derived DN2 cells found at 1 mo after transplant, these results indicate that in this competitive setting, *Lmo2*-transgenic LMPPs can generate a population of developmentally blocked DN2 thymocytes that persist long term but do not expand in number, suggesting that these cells lack self-renewal capacity.

Acquisition of long-term engraftment potential in *Lmo2*-transgenic thymocytes correlates with phenotypic evolution and TCR-β rearrangement

We have previously shown that thymocytes in adult (2 mo old) *Lmo2*-transgenic mice have self-renewal potential, as evidenced by serial long-term engraftment in transplantation experiments, and that this capacity is restricted to DN3 thymocytes (McCormack et al., 2010). To determine the stage at which long-term engraftment capacity arises in these mice, we transplanted thymocytes from *Lmo2*-transgenic mice of various ages into sublethally irradiated congenic (CD45.1) recipients (Fig. S2 A). This showed that while thymocytes from 1-wk-old *Lmo2*-transgenic mice did not engraft long-term (Fig. S2 B), and thymocytes from 1-mo-old *Lmo2*-transgenic mice showed variable engraftment potential, thymocytes from 2-mo-old *Lmo2*-transgenic mice showed near-complete long-term engraftment of recipient thymi, as shown previously (McCormack et al., 2010; Fig. S2 B). Further analysis of donor thymocytes from 1- and 2-mo-old *Lmo2*-transgenic mice showed that they comprised all T cell subsets after the DN3 stage (Fig. S2, C and D), suggesting that DN3 thymocytes are the source of long-term engrafting cells, as shown previously (McCormack et al., 2010).

The presence of long-term engrafting thymocytes from 1–2 mo of age implies that their development is a frequent event in *Lmo2*-transgenic mice. Accordingly, assessment of TCR-β subfamily usage showed that at 1 wk of age, *Lmo2*-transgenic T cells were polyclonal; however, by 2 mo of age dominant clones arose, suggesting the possible presence of secondary mutations in enabling thymocyte self-renewal (Fig. S2 E). Moreover, sorted DN3a thymocytes from 2-mo-old *Lmo2*-transgenic mice showed the presence of multiple clones with distinct TCR-β usage, which were maintained when these cells were transplanted (Fig. S2, F–I). Thus, the acquisition of long-term engraftment potential in *Lmo2*-transgenic thymocytes is a frequent event, often occurring in multiple clones by 2 mo of age.

Restored thymocyte competition abrogates *Lmo2*-driven T-ALL

Previous studies have shown increased apoptosis in pre-LSCs that arise in *Lmo2*-transgenic mice from 6 wk of age (Tremblay et al., 2016). To determine whether this also occurs in developmentally arrested DN2 thymocytes in young *Lmo2*-transgenic mice, we analyzed the apoptosis of *Lmo2*-transgenic mice at 2 wk of age. We found a marked increase in apoptotic cells specifically within the developmentally arrested DN2 population (Fig. 4, A–C), suggesting that apoptosis is a critical mediator of the defect in cellular competition that drives the development of pre-LSCs in *Lmo2*-transgenic mice. To test this further, we bred *Lmo2*-transgenic mice with *Vav-BCL2* transgenic mice that express the antiapoptotic factor BCL2 throughout hematopoiesis (Ogilvy et al., 1999). This led to a restoration of thymus size in *Lmo2*-transgenic mice (Fig. S3 A), and while DN thymocytes still accumulated in *Lmo2;BCL2* double transgenic mice, these included not only the DN3a cells that accumulate in *Lmo2*-transgenic mice but downstream DN3b-c and DN4 subsets as well (Fig. S3, B and C). Accordingly, in competitive BM transplantation experiments, BCL2 expression restored the contribution of *Lmo2*-transgenic cells to the DN3 and DN4 stages (Fig. S3, D–F). However, development of double-positive (DP) and CD4/CD8 single-positive (SP) T cells remained significantly impaired, in line with previous findings that DP cells are reduced in *BCL2*-transgenic mice (Ogilvy et al., 1999).

Cell cycle analysis of *Lmo2;BCL2* double transgenic thymocytes showed that DN3 cells in these mice were mostly quiescent (Fig. S4 A), and there was no evidence of expanded T cell clones, implying that pre-LSCs do not emerge in the thymi of these mice (Fig. S4 B). Accordingly, in long-term engraftment experiments, while both *BCL2*-transgenic and *Lmo2;BCL2* double transgenic thymocytes showed some engraftment in primary recipients (Fig. S4, C–E), this was not maintained in secondary recipients, unlike *Lmo2*-transgenic thymocytes, which show serial transplantation capacity (Fig. S4, C, F and G; McCormack et al., 2010). Moreover, onset of T-ALL in these mice was almost completely abrogated (Fig. 4 D), with *Lmo2;BCL2* double transgenic mice instead succumbing to B cell neoplasms similar to those seen in *BCL2*-transgenic mice (Egle et al., 2004; Fig. 4, E–G). Thus, BCL2 rescues the failure of cell competition in the thymus of *Lmo2*-transgenic mice, thereby preventing the development of pre-LSCs and subsequent leukemogenesis.

To determine whether competition from WT progenitors could similarly prevent *Lmo2*-driven leukemogenesis, we performed BM transplantation experiments in which *Lmo2*-transgenic BM cells were injected with or without a 1:3 ratio of WT competitor cells. While mice transplanted with *Lmo2*-transgenic BM cells in the absence of competitor developed leukemia at a similar rate to *Lmo2*-transgenic mice (Fig. 5 A, compare with Fig. 4 D) in the presence of WT BM cells, T-ALL initiation was almost completely overcome, with only three of 11 mice analyzed succumbing to T-ALL with long latency (Fig. 5, A, C and D), despite robust hematopoietic engraftment (Fig. 5 B). At endpoint, a

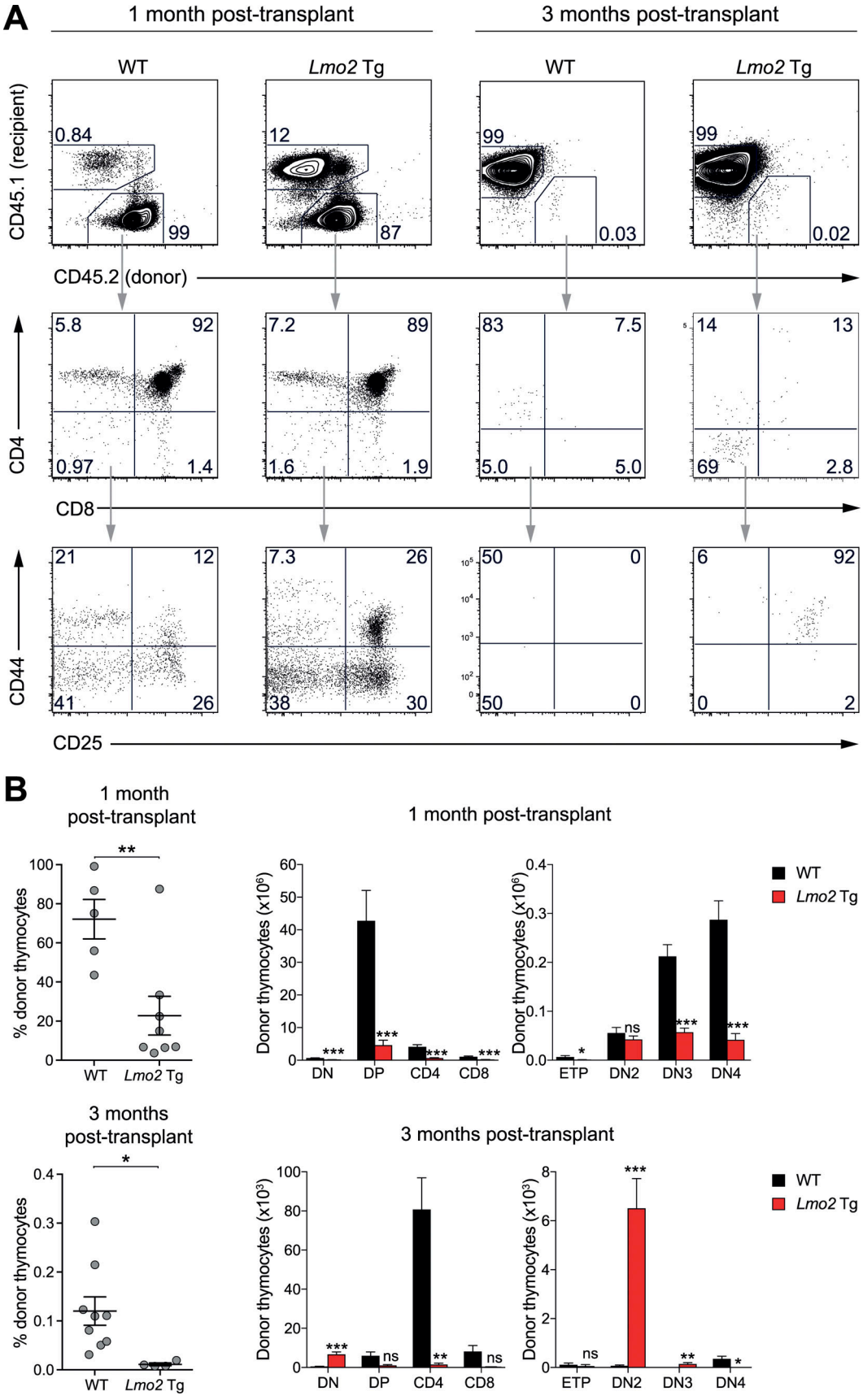

Figure 3. ***Lmo2*-transgenic DN2 thymocytes persist long-term but do not expand in vivo.** LMPPs were FACS sorted from CD45.2 WT or CD45.2 *Lmo2*-transgenic (Tg) mice and injected directly into the thymi of sublethally irradiated (650 rad) CD45.1 WT recipient mice. Thymi were then harvested at 1 and 3 mo

after transplant and donor/recipient cell contribution was determined. **(A)** Representative flow cytometric analysis of thymi from recipient mice at the indicated time points. **(B)** Percentage of donor thymocytes (left; points show individual recipient mice and lines show mean ± SEM) and number of donor thymocytes in each *T* cell subset (center, right; data are mean + SEM) in recipient mice as in A at 1 and 3 mo after transplant. Data are from two to three separate experiments. *P < 0.05, **P < 0.01, and ***P < 0.001 compared with WT controls (Student's *t* test).

further four mice receiving *Lmo2*-transgenic BM cells plus competitor contained small thymi containing donor cells that were blocked at the DN2 stage (data not shown), while the remainder (four of 11) were athymic. Therefore, impaired cell competition is required for *Lmo2*-driven T cell leukemogenesis.

Molecular features of developmentally arrested thymocytes in *Lmo2*-transgenic mice

To examine the molecular features of developmentally arrested thymocytes in *Lmo2*-transgenic mice, we used RNA sequencing (RNA-seq) to compare the gene expression profiles of *Lmo2*-transgenic DN2 and DN3 thymocytes at two separate time points, 2–3 wk of age (hereafter termed "young"), a point at which developmentally arrested DN2 thymocytes are present but pre-LSCs have not yet arisen, and 6–10 wk of age (hereafter termed "old"), at which point self-renewing DN3 thymocytes (pre-LSCs) have developed. Multidimensional scaling showed that the greatest transcriptional changes were in young DN2 thymocytes, with *Lmo2*-transgenic DN3a thymocytes being more closely related to WT cells, before diverging in older mice (Fig. 6 A and Table S1). Analysis of *Lmo2* expression confirmed its overexpression in all three *Lmo2*-transgenic thymocyte populations analyzed (Fig. 6 B). Gene set analysis showed that genes that are normally upregulated during the transition from ETP to DN2 thymocytes remained repressed in young *Lmo2*-transgenic DN2 thymocytes (Fig. 6 C), including *Ptcra*, *CD3d*, *CD3e*, *CD3g*, *IL7r*, and *Rag1* (Table S2). Furthermore, genes normally downregulated during the ETP to DN2 transition remained expressed in these cells (Fig. 6 C), including HSC-associated (*Cd34*, *Hhex*) and myeloid-associated genes (*Mpo*, *Gfi1b*; Table S2). Moreover, as expected from our finding that these cells are quiescent (Fig. S1, D and E), genes involved in the cell cycle were strongly downregulated (Fig. 6 D). Thus, developmentally arrested *Lmo2*-transgenic DN2 thymocytes show a gene expression profile that is reminiscent of ETPs.

Similar gene set analyses of old, self-renewing DN3a thymocytes showed that these cells also showed an immature gene expression profile, similar to normal DN2 thymocytes (Fig. 6 E). Moreover, cell cycle genes were upregulated (Fig. 6 F), indicating a high degree of cell cycling in this population, which could account for the acquisition of further mutations that promote overt leukemogenesis.

Identification of early and late-acting mutations in *Lmo2*-driven murine T-ALL

Our results demonstrate that failure of cell competition in *Lmo2*-transgenic thymocytes promotes mutations that result in development of pre-LSCs, which are then complemented by further mutations en route to overt leukemogenesis. To explore the nature of these cooperating genetic events, we serially transplanted thymocytes from preleukemic (8–10 wk old) *Lmo2*-transgenic mice into irradiated recipients, with secondary recipients then left to develop leukemia (Fig. 7 A). Exome sequencing was then performed using tail DNA (as a germline reference), preleukemic thymocytes ($n = 4$), and leukemia derived from secondary transplants ($n = 17$ in total from two donors). These data were then analyzed to determine (i) the genomic landscape of *Lmo2*-induced T cell leukemia and (ii) the ontogeny of secondary mutations to distinguish early- and late-arising events. Notably, secondary transplant recipients developed leukemia at a rate comparable with that arising in *Lmo2*-transgenic mice (Fig. 7 B).

Analysis of genomic copy number alterations (CNA) revealed trisomy of chromosome 15 and loss of inactive X chromosome in *Lmo2*-transgenic thymi, which persisted into the derivative leukemias (Fig. 7 C). While these were the only chromosome-level CNAs in *Lmo2*-transgenic thymocytes, leukemias acquired additional chromosomal changes including trisomy of chromosomes 11 and 14 (Fig. 7 C).

Single nucleotide variant (SNV) analysis revealed few mutations in the *Lmo2*-transgenic thymi (median 18, range 7–25) and an increased frequency in derived leukemias (median 33, range 3–62; for example, Fig. 7 D). This also revealed interesting details regarding the timing of *Notch* mutations in this model. Subclonal insertion mutations in exon 34 of *Notch1* were found in three of four *Lmo2*-transgenic thymocyte samples (Fig. 7 E) and increased in penetrance in leukemias (Fig. 7, D and E). These caused frameshift mutations in the PEST domain, loss of which causes stabilization of NOTCH1 protein but not constitutive activation (Koch and Radtke, 2011). Moreover, donor 4 contained two clones with distinct mutations, each giving rise to a subset of derivative leukemias (Fig. 7 E). In addition to exon 34 mutations, four mutations were detected in exon 26/27 of *Notch1*, which encodes the heterodimerization domain, across six leukemias (Fig. 7 E). These mutations are thought to cause constitutive receptor activation (Koch and Radtke, 2011), and in contrast to exon 34 mutations, these were absent in preleukemic thymocytes.

In addition to *Notch1*, two other genes were recurrently mutated: *Trp53* and *Pten*, both of which are established tumor suppressors in human T-ALL (Liu et al., 2017). In all, 12 different *Trp53* mutations were detected across 10 leukemias, and in many cases, the variant allele frequency exceeded 50%, indicating loss of the WT allele (Fig. 7, D and E). *Pten* mutations were detected in three leukemias, and a further two had evidence of focal copy number loss (Fig. 7, E and F). Like *Notch1* exon 26/27 mutations, *Trp53* and *Pten* mutations were absent in donor thymocytes and mostly unique, implying that they were acquired late during oncogenesis.

These results imply that exon 34 *Notch1* mutations are a feature of pre-LSCs in this model. To further analyze this, we

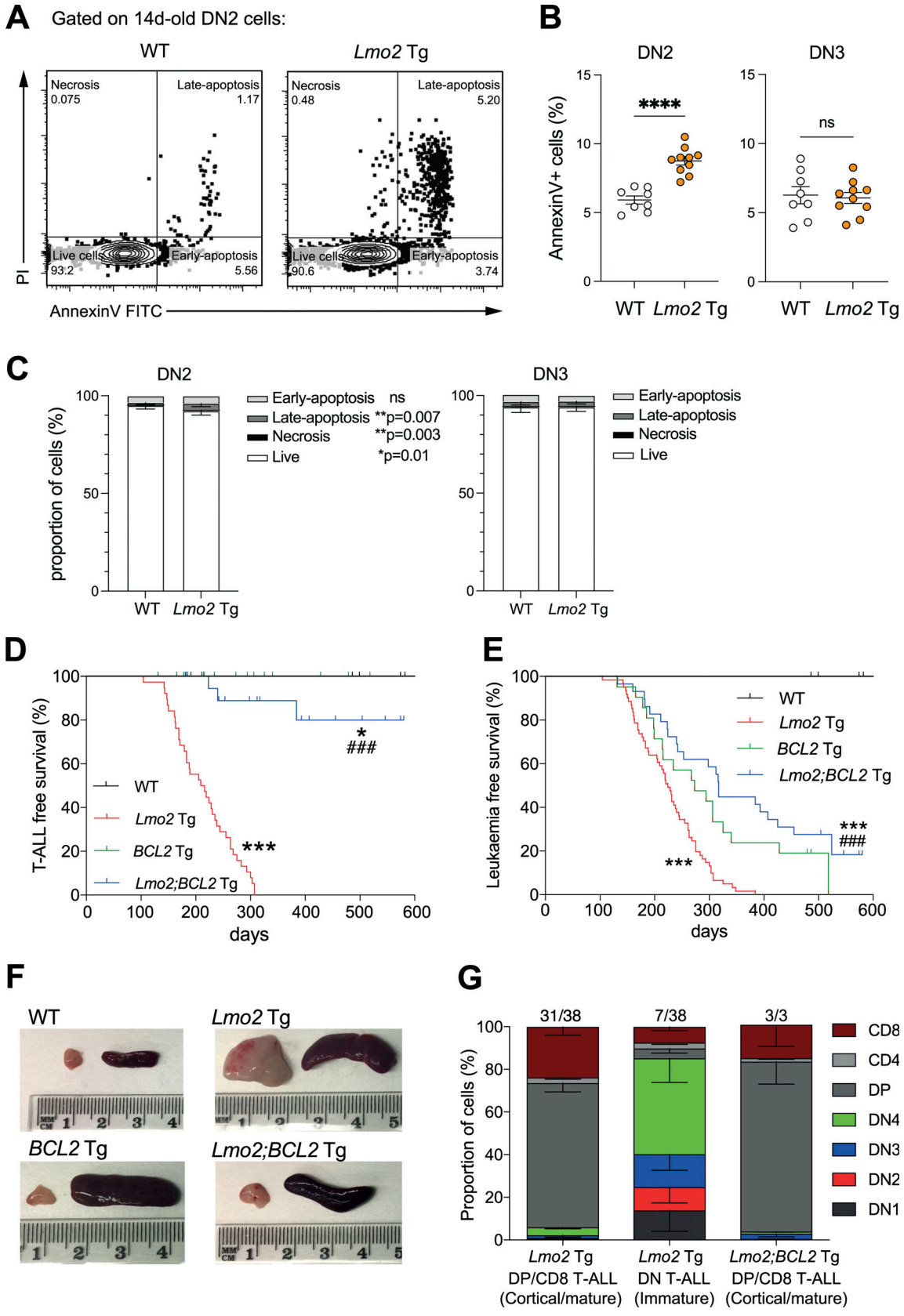

Figure 4. **BCL2 overexpression inhibits *Lmo2*-driven T-ALL. (A–C)** Increased apoptosis in *Lmo2*-transgenic DN2 thymocytes. **(A)** Representative Annexin-PI flow cytometric analysis of DN2 thymocytes from WT and *Lmo2*-transgenic (Tg) mice at 14 d. Gating of live cells, early apoptosis, late apoptosis, and necrosis are shown. **(B)** Percentage of Annexin V positive DN2 and DN3 thymocytes in WT and *Lmo2*-transgenic mice. Points show individual mice and lines are mean ± SEM. Data are from two separate experiments. ****P < 0.0001. **(C)** Quantification of apoptosis stages in DN2 and DN3 from each group measured by flow

cytometry as shown in A. *n* = 8-10 mice per group. Results are mean – SEM. *P < 0.05, **P < 0.01 compared to WT (Student's *t* test). **(D and E)** Kaplan-Meier curves of T-ALL-free (D) and overall (E) survival of WT (*n* = 19), *Lmo2* (*n* = 61), *BCL2* (*n* = 21), and *Lmo2;BCL2* (*n* = 29) transgenic mice. *P < 0.05, ***P < 0.001 vs. WT, ###P < 0.001 vs. *Lmo2* transgenic (Log-rank Mantel-Cox test). **(F)** Images of thymi and spleens from mice of the indicated genotypes that were culled due to illness or had reached experimental endpoint (WT). **(G)** Immunophenotypes of T-ALLs (from thymi or spleen) from *Lmo2* transgenic and *Lmo2;BCL2* double transgenic mice, classified as cortical/mature (DP/CD8 T-ALL) or immature (DN T-ALL). Numbers above indicate the number of mice displaying the indicated T-ALL phenotype relative to the total number of mice analyzed. Data are mean – SEM.

studied our previously acquired RNA-seq data from *Lmo2*-transgenic pre-LSCs (Fig. 6). This showed that exon 34 *Notch1* mutations were also seen in pre-LSCs from three separate mice and increased in penetrance upon transplantation (Fig. S4 H). In contrast, Notch mutations were not seen in DN3a thymocytes from two *Lmo2;BCL2* double transgenic mice (Fig. S4 H). These results imply a model whereby impaired cell competition promotes the selection of stabilizing mutations in the *Notch1* PEST domain that facilitates the development of pre-LSCs (Fig. 7 G). These are then complemented by further mutations in tumor suppressors (in particular *Pten* and *Trp53*) to facilitate the development of overt leukemia.

Discussion

Cellular self-renewal is a key driver of cancer progression. Whilst LMO2 is one of a group of oncogenic T-ALL–causing transcription factors that can transform thymocytes into self-renewing pre-LSCs (Gerby et al., 2014; McCormack et al., 2010; Shields et al., 2019), the cellular and molecular events leading to the development of pre-LSCs in *Lmo2*-transgenic mice were unclear.

In our previous studies, we used a lineage-tracing approach to show that thymic import from the BM was impaired from an early age (McCormack et al., 2010). Together with our findings that *Lmo2*-transgenic thymocytes possessed serial transplantation capacity from a young age, this led us to conclude that LMO2 directly induced self-renewal of thymocytes and that these self-renewing pre-LSCs then blocked the import of thymus-settling progenitors (Curtis and McCormack, 2010; McCormack et al., 2010). In contrast, here we have used a combination of neonatal thymus transplantation, competitive BM transplantation, and intrathymic transplantation of LMPPs to show that *Lmo2*-transgenic thymocytes do not initially show long-term engraftment/self-renewal capacity, but rather show a severe block at the DN2 stage of T cell development. These developmentally arrested cells are quiescent and show an ETP-like gene expression profile, but do not expand in vivo nor show long-term engraftment capacity. However, the developmental arrest of these DN2 cells results in a failure of downstream cell competition, which promotes outgrowth of cells with genomic abnormalities, including Trisomy 15 and *Notch1* PEST domain mutations, resulting in the emergence of self-renewing pre-LSCs (Fig. S5). This selection/mutation process is remarkably rapid, inevitably leading to the development of one or more populations of clonally expanded pre-LSCs that are developmentally arrested at the DN3a stage, show long-term engraftment capacity, and are marked by rearranged TCR-β subunits by 2 mo of age. These pre-LSCs then acquire further mutations, in particular loss or mutation of tumor suppressor genes including *Pten* and *Trp53*, leading to overt leukemia.

Our results are reminiscent of studies showing that impaired cell competition in the thymus can result in thymocyte self-renewal (Boehm, 2012; Martins et al., 2012; Peaudecerf et al., 2012) and that this can cause T cell leukemogenesis (Martins et al., 2014). More recent studies have examined the consequences of failed thymocyte competition in the setting of impaired progenitor import (Ramos et al., 2020), identifying an abnormal population that is the putative cell-of-origin of leukemia in this setting (Paiva et al., 2021). It will be interesting to determine whether a similar cell population arises in the thymi of *Lmo2*-transgenic mice to give rise to pre-LSCs.

Recently, a similar mechanism of impaired cellular competition leading to leukemia was found to occur in a mouse model of gene therapy for X-SCID (Ginn et al., 2017; Ginn et al., 2010; Ginn et al., 2018). As *LMO2* was preferentially targeted by retroviral insertion in gene therapy trials for X-SCID (Hacein-Bey-Abina et al., 2008; Hacein-Bey-Abina et al., 2003; Howe et al., 2008; McCormack and Rabbitts, 2004), our results imply that the resultant LMO2 overexpression may have exacerbated the accumulation of developmentally arrested progenitors in the thymi of these patients, as well as promoting self-renewal of downstream progenitor populations in conjunction with *NOTCH1* mutations.

These findings have implications for the ontogeny of T-ALL in humans, which in the majority of cases appear to evolve from pre-LSCs (Roels et al., 2020). They indicate that LMO2 is insufficient to initiate self-renewal of pre-LSCs, as assumed previously (Cleveland et al., 2013; Curtis and McCormack, 2010; McCormack and Curtis, 2010), but can facilitate as well as cooperate with mutations in *Notch1* to do so (Fig. S5). As such, overexpression of LMO2 can contribute to leukemogenesis either as an initiating event, as in *Lmo2*-transgenic mice, or insertional activation during X-SCID gene therapy trials or as a secondary event, as was seen in the setting of progenitor deprivation (Martins et al., 2014), in which LMO2 was upregulated late during leukemogenesis following thymus autonomy.

Notch1 mutations have been previously reported in transgenic mouse models of T-ALL (Göthert et al., 2007; Lin et al., 2006), and it has been suggested that these occur in the preleukemic phase (Tatarek et al., 2011), in line with leukemia-associated *NOTCH1* alleles being weak tumor initiators (Chiang et al., 2008). Using exome sequencing, we show that in *Lmo2*–transgenic mice, Notch1-stabilizing (PEST domain) mutations occur in the preleukemic phase; however activating (transmembrane) mutations occur late during oncogenesis. In human T-ALL however, *NOTCH1* mutations have been found to occur either as early (prenatal) or as late events (Eguchi-Ishimae et al.,

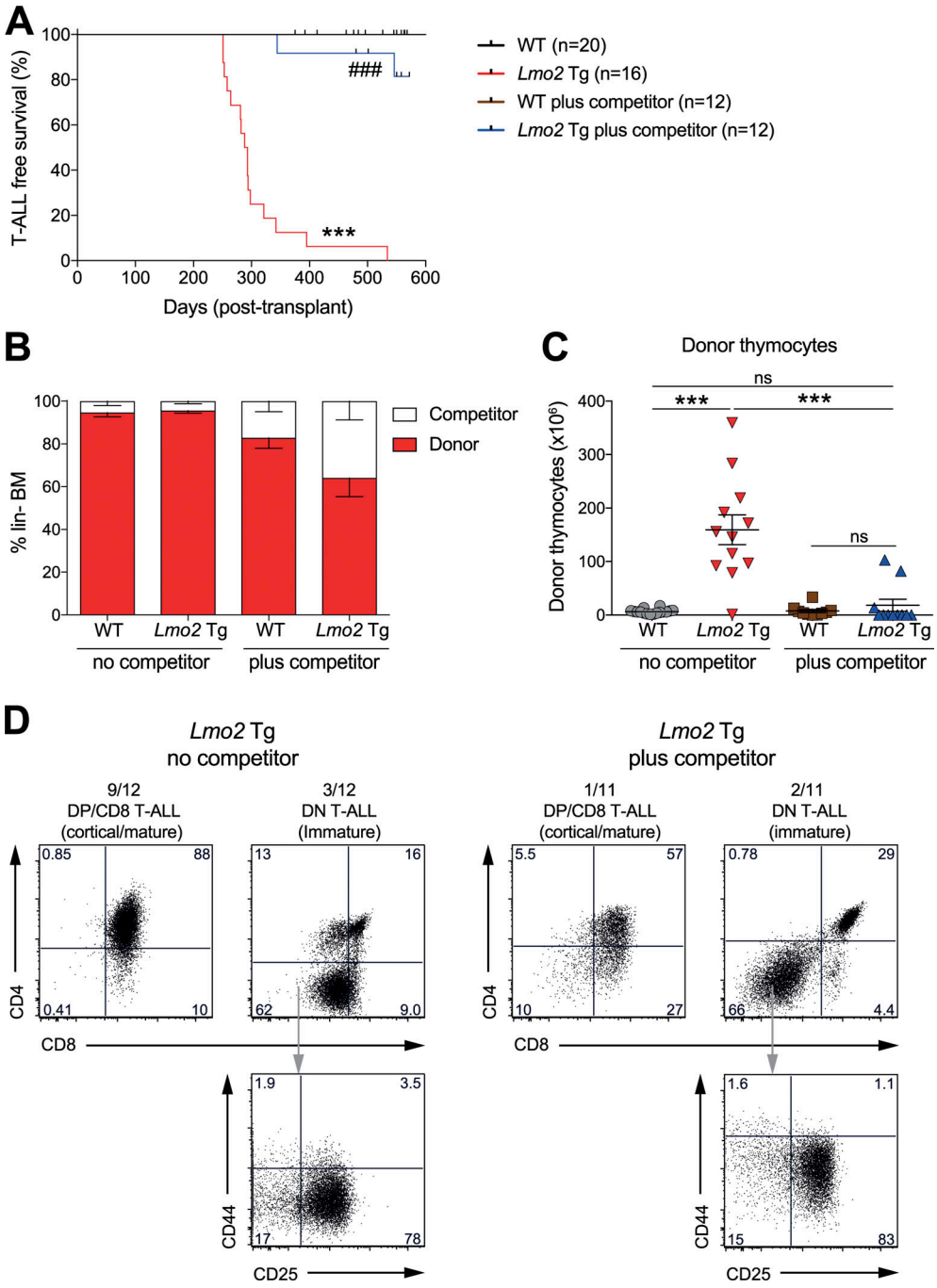

Figure 5. **Thymic competition inhibits *Lmo2*-induced T-ALL. (A)** Kaplan–Meier survival curve of mice transplanted with WT and *Lmo2*-transgenic (Tg) BM cells with or without a 1:3 ratio of WT congenic (CD45.1) competitor cells. ***P < 0.001 vs. WT, ###P < 0.001 vs. *Lmo2*-transgenic. Data are combined from two to four independent experiments. **(B)** Percentage of donor/competitor cell contribution in BM of mice that either succumbed to T-ALL or were sacrificed at experimental endpoint. Data are mean – SEM of *n* = 10–15. **(C)** Number of donor thymocytes from mice that either succumbed to T-ALL or were sacrificed at experimental endpoint. Points show individual mice and lines show mean ± SEM. ***P < 0.001 (Student's *t* test). **(D)** FACS analysis of thymocytes from representative leukemic mice transplanted with *Lmo2*-transgenic BM with and without competitor. Numbers at the top indicate the number of mice displaying the indicated leukemic phenotype relative to the total number analyzed.

2008; Mansour et al., 2007). Irrespective of the order of mutation, our studies indicate that cooperation of the LMO2 and NOTCH pathways is essential to facilitate the development of self-renewing pre-LSCs that can initiate T-ALL.

We have recently used a repressible model of LMO2 overexpression to demonstrate that continued expression of LMO2 is essential for survival and self-renewal of pre-LSCs in vivo (Abdulla et al., 2021). Thus, LMO2 drives a self-renewal program that is essential for pre-LSC self-renewal but requires additional mutations, perhaps to allow cell survival. In contrast to pre-LSCs, we and others have found that overt leukemia stem cells (LSCs) in LMO2-driven T-ALL models often do not require

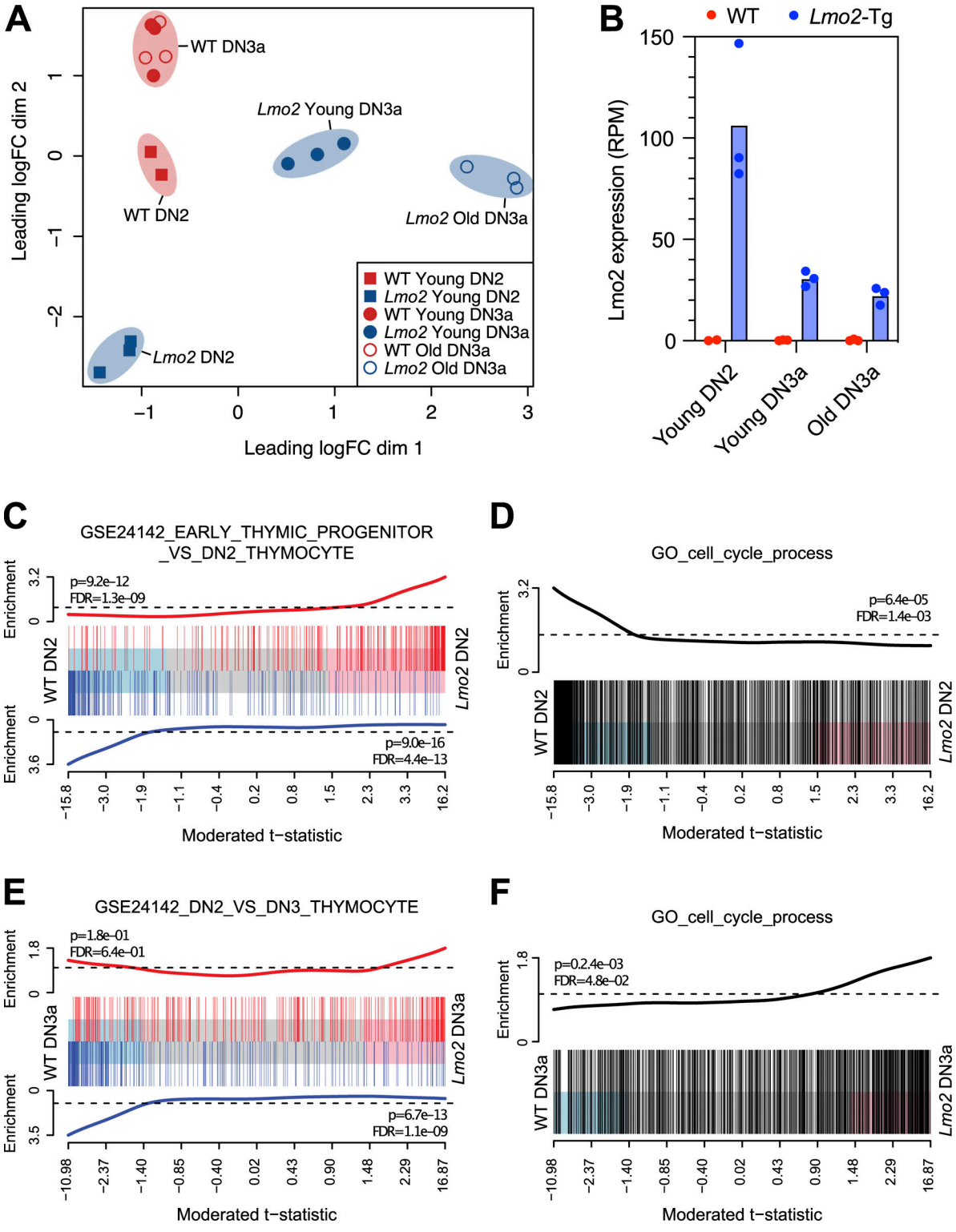

Figure 6. **Gene expression profiles of *Lmo2*-transgenic thymocyte populations. (A)** Multidimensional scaling plot of RNA-seq data showing the association between WT and *Lmo2*-transgenic (*Lmo2*) DN2 and DN3a thymocytes. Young thymocytes were derived from 2–3-wk-old mice while old thymocytes were from 6–10-wk-old mice. **(B)** Gene expression of *Lmo2* in the indicated populations of WT and *Lmo2*-transgenic (Tg) mice, from RNA-seq data as in A. Bars show the mean. Data are reads per million mapped reads (RPM). **(C)** Gene set enrichment plot showing upregulation of ETP genes in *Lmo2*-transgenic DN2 thymocytes from young (2–3 wk old) mice. RNA-seq differential gene expression between *Lmo2*-transgenic and WT DN2 thymocytes is shown as a shaded rectangle with genes horizontally ranked by moderated t-statistic. Blue and pink shades of the rectangle represent up and downregulation of genes, respectively, in *Lmo2*-transgenic compared to WT. Overlaid bars are a previously described set of genes upregulated (red bars) and downregulated (blue bars) in ETPs vs. DN2 thymocytes (from Belyaev et al., 2012). Red and blue worms above and below represent the relative enrichment. P values and false dicovery rates (FDRs) were computed by the camera method (Wu and Smyth, 2012). **(D)** Enrichment plot and test results as in C, for Gene Ontology (GO) cell cycle process

genes. Skewing to the left indicates downregulation of cell cycle genes in *Lmo2*-transgenic young DN2 thymocytes. **(E)** Gene set enrichment plot showing upregulation of DN2 genes in *Lmo2*-transgenic DN3a thymocytes from old mice. Red and blue overlaid bars represent genes upregulated and downregulated, respectively, in DN2 vs. DN3 thymocytes (from Belyaev et al., 2012). **(F)** Enrichment plot and test results as in C, for GO cell cycle process genes. Skewing to the right indicates upregulation of cell cycle genes in *Lmo2*-transgenic DN3a thymocytes.

LMO2 for sustained self-renewal, indicating that subsequent mutations or epigenetic events overcome the requirement of LMO2 (Abdulla et al., 2021; García-Ramírez et al., 2018). In particular, we found loss of the tumor suppressor *Ikaros* can do so (Abdulla et al., 2021). In this study, no mutations were found in *Ikaros*; however, additional mutations in tumor suppressors (*Pten* and *Trp53*) were found. As loss of either of these tumor suppressors could not directly enable the transition to LMO2 independence (Abdulla et al., 2021), it will be interesting to determine whether leukemias in the *CD2-Lmo2* transgenic model used here are also LMO2-independent and if so, to define the molecular mediators of this process.

An interesting finding of this study is that the presence of WT progenitors in the thymus can potently inhibit *Lmo2*-driven T cell leukemogenesis (Fig. 5). This implies that *Lmo2* overexpression in a majority of T cell progenitors is necessary to impair cell competition and promote T-ALL (Fig. S5). Indeed, ubiquitous expression of a transgene within one or more lineages is a general feature of transgenic mouse models, which may impair cell competition and promote oncogenesis as shown here. In contrast, during retroviral transduction/transplantation studies, transduction is incomplete, thus it is interesting that LMO2 can also cause leukemogenesis in this setting (Sincennes et al., 2016; Treanor et al., 2011). However, retroviral vectors can cause retroviral insertion mutagenesis, which can itself cause a developmental block at the DN2 stage (Zhou et al., 2016). Thus, either increased expression of LMO2, caused by retroviral overexpression, or activation of cooperating genes by insertion mutagenesis may facilitate leukemogenesis in these studies.

In addition to WT progenitors, we found that overexpression of the antiapoptotic factor BCL2 potently inhibited the emergence of pre-LSCs containing *Notch1* mutations and subsequent T-ALL development. This correlated with complete restoration of the DN3-4 compartment in competitive BM transplant assays, supporting previous studies that showed that DN3 is the major stage at which cell competition occurs in the thymus to prevent T cell leukemogenesis (Martins et al., 2014). Together with our finding of increased apoptosis in DN2 thymocytes in *Lmo2*-transgenic mice, this implies that a key role of secondary mutations, in particular in the *Notch1* pathway, is to overcome LMO2-induced thymocyte apoptosis and allow the development of self-renewing pre-LSCs that are the origin of leukemia in this model (Fig. S5). Indeed, thymocyte apoptosis is also induced by the related transcription factors TAL1 and LMO1 as a prelude to leukemia (Herblot et al., 2000; Shank-Calvo et al., 2006) and is also a key mediator of thymic lymphoma caused by γ-irradiation (Michalak et al., 2010). These findings also imply that therapies that induce thymocyte apoptosis may inadvertently promote T-ALL.

In summary, we have found that impaired cell competition is critical for the emergence of pre-LSCs and subsequent leukemogenesis in a transgenic mouse model of T-ALL, implying that this process may play a role in human T-ALL leukemogenesis. Notably, the effects of impaired competition on downstream thymocyte populations are starting to be appreciated (Martins et al., 2014; Paiva et al., 2021; Ramos et al., 2020), and it will be interesting to determine how these processes cooperate with oncogenic transcription factors to cause leukemia in transgenic mouse models as well as human T-ALL.

Materials and methods

Mice

CD2-Lmo2 (Larson et al., 1994) and *Vav-BCL2* (Ogilvy et al., 1999) transgenic mice were maintained on a C57BL/6 background. WT C57BL/6 mice (CD45.1 or CD45.2) were supplied by Walter and Eliza Hall Institute (WEHI) Bioservices. All procedures were approved by WEHI Animal Ethics Committee.

Transplantation assays

For thymocyte transplantation assays, C57BL/6 (CD45.1) congenic recipient mice were sublethally irradiated (6.5 Gy) and injected via the tail vein with thymocytes equivalent to one-quarter of the thymus as described previously (McCormack and Curtis, 2010).

For BM transplantation assays C57BL/6 (CD45.1), congenic recipient mice were lethally irradiated (9.5 Gy) and injected intravenously with 10^7 BM cells (CD45.2). For competitive BM transplantation assays, mice received test BM and WT BM (CD45.1) at a 3:1 ratio.

For intrathymic transplantation assays, C57BL/6 (CD45.1) recipients were sublethally irradiated (6.5 Gy), anesthetized, and intrathymically injected with 5,000 sorted LMPPs.

Flow cytometry

Cells were stained using fluorophore-conjugated antibodies purchased from either eBiosciences, Biolegend, BD Pharmingen, or WEHI Monoclonal Antibody Production Facility. For lineage depletion, BM cells were stained with biotinylated anti-CD2, CD3, Thy1.2, Gr1, Ter119, B220, CD19, and Mac1 and depleted using MACS LS columns (Miltenyi Biotec). To distinguish apoptotic/necrotic cells in stained samples, FITC Annexin V and propidium iodide (final concentration of 2.5 µg/ml) were added 1–10 min prior to acquiring the data. For cell cycle analysis, cells were fixed and permeabilized using Cytofix/Cytoperm (BD Pharmingen) and then stained with anti-Ki67 FITC (B56; BD) and 10 µg/ml DAPI. TCR Vß-subfamily usage was assessed using the Mouse Vß TCR Screening Panel (BD Pharmingen). Cells were analyzed on an LSR Fortessa or FACSymphony A3 (BD) and sorted on a FACS Aria II (BD). Data were analyzed using FlowJo (Treestar; version 9.9.5).

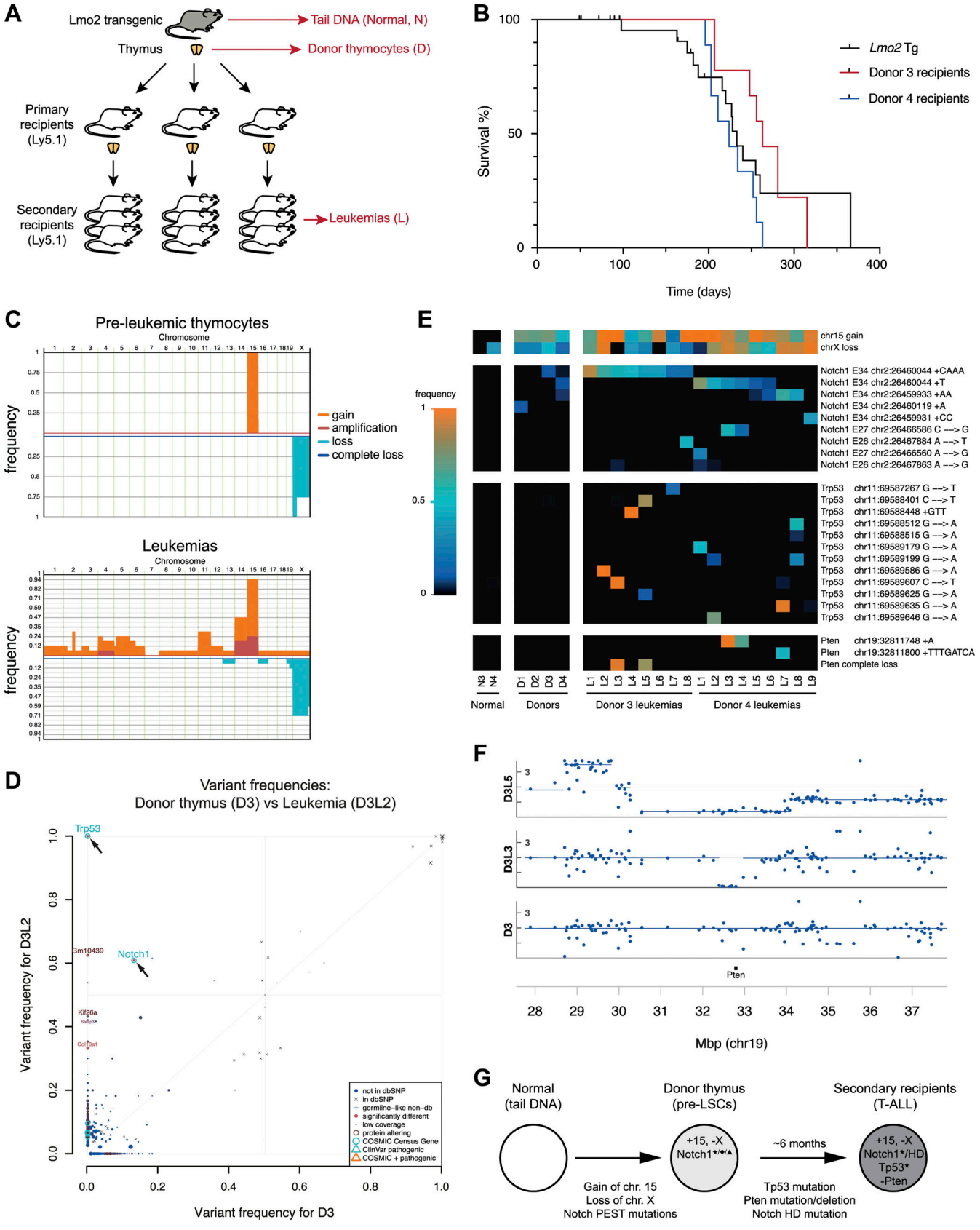

Figure 7. **Analysis of early- and late-arising mutations during *Lmo2*-driven T cell leukemogenesis. (A)** Strategy to identify secondary mutations in *Lmo2*-induced pre-LSCs and derivative leukemias. Two independent populations of *Lmo2*-transgenic (Tg) thymocytes were transplanted into CD45.1 mice and 1 mo later donor cells were harvested and re-transplanted into secondary CD45.1 recipient mice that were monitored until development of leukemia. DNA was

collected from the tail of donor mice (normal), from pre-leukemic thymocytes (donor) and leukemias from secondary transplant mice (leukemia) for exome sequencing. **(B)** Kaplan–Meier survival curves of secondary recipient mice receiving thymocytes from Donors 3 and 4, compared with unmanipulated *Lmo2*-transgenic mice. For secondary recipients, the survival curve is adjusted to account for age of donor mice (8–10 wk). **(C)** Summary of large-scale (>20 Mb) CNAs in *Lmo2*-transgenic preleukemic thymi (top, n = 4) and leukemias (bottom, n = 17). Genomic regions with gain, amplification, loss, or complete loss are distinguished by color. A threshold of >25% clonality was applied and the Y chromosome was excluded. **(D)** Scatter plot showing Variant Allele Frequency (VAF) of SNVs in *Lmo2*-transgenic Donor #3 thymocytes and a derivative leukemia (D3L2). Point type reflects variant classification, with size proportional to read depth. Mutations in *Notch1* and *Trp53* are marked. dbSNP, the Single Nucleotide Polymorphism Database. **(E)** Heat map showing the clonality of chromosomal copy number changes (top) and VAF of coding mutations in donor tail DNA (N3, N4), donor thymocytes (D1–4), and derived leukemias (L). **(F)** SuperFreq absolute copy number surrounding the *Pten* gene, showing focal loss in two leukemias. Lines show segmentation and consensus copy number and dots show estimated copy number of individual genes. **(G)** Summary of secondary events occurring in *Lmo2*-driven T cell leukemia. Chromosomal abnormalities and recurrent mutations occurring in pre-LSCs vs. T-ALL are shown. For Notch1, individual symbols indicate multiple mutations present at low frequency in the donor thymus, one of which became fixed upon transplantation and subsequent leukemogenesis. Chr., chromosome.

RNA-seq and analysis

RNA was extracted using RNeasy Plus Micro (Qiagen) and analyzed using a 2200 Tapestation Analyser (Agilent). Libraries were then generated using TruSeq RNA Library Prep v2 (Illumina). Sequencing was performed on a HiSeq 2000 (Illumina) to produce 100-bp single-end reads. Between 7 and 12 million reads were generated for each sample, and reads were aligned to the *Mus musculus* genome (mm10) using Rsubread (Liao et al., 2019). The number of reads overlapping mouse Entrez genes was summarized using featureCounts and Rsubread's built-in National Center for Biotechnology Information gene annotation. Low expressed genes were filtered if they failed to achieve at least 0.5 counts per million in at least three libraries. Genes without annotation were also filtered. Differential expression analyses were undertaken using the edgeR (Robinson et al., 2010) and limma (Ritchie et al., 2015) software packages. Library sizes were normalized using the trimmed mean of M-values method (Robinson and Oshlack, 2010). Log2 fold-changes were computed using Voom (Law et al., 2014). Differential expression was assessed relative to a fold change threshold of 1.5 using TREAT (McCarthy and Smyth, 2009). The false discovery rate was controlled below 0.05 using the method of Benjamini and Hochberg. Barcode plots illustrating the enrichment of interested pathway genes were drawn using limma's barcode plot function. Gene set enrichment tests used the camera method (Wu and Smyth, 2012).

Analysis of *Notch1* mutations was performed using *Integrative Genomics Viewer* (Broad Institute) version 2.4.

Exome sequencing and analysis

Genomic DNA was extracted using the AllPrep DNA/RNA Mini kit (Qiagen) and analyzed with the Bioanalyzer DNA 1000 chip (Agilent 2200; TapeStation instrument). DNA libraries were prepared from 100 ng DNA using SureSelectXT2 Reagent kit (Agilent) with purifications between steps carried out with Agencourt AMPure XP beads. Library yields were estimated with the Qubit dsDNA HS kit (Invitrogen). Hybridization of pooled libraries to capture probes and removal of nonhybridized molecules were then carried out. Targeted regions were amplified, producing sequence-ready libraries that were sequenced on an HiSeq 2000 sequencer (Illumina) at the Australian Genome Research Facility.

The sequenced libraries were aligned to mm10 using Burrows-Wheeler Alignment (Li and Durbin, 2009), resulting in a mean read depth of 29× (range 6–59×) over the capture regions for the cohort. Preliminary variant calling was carried out with Varscan2 (Koboldt et al., 2012). SuperFreq (Flensburg et al., 2020) was used for somatic SNV and CNA calling and for tracking mutations across samples. Two normal control (tail DNA) samples were used to designate germline and somatic variants. Somatic mutation profiles were used to match leukemia samples with donors. Leukemias were designated Donor 3 (D3 L1–L8) or Donor 4 (D4 L1–L9) based on clustering, with one sample removed due to poor quality. To assess mutation load, we considered variants with SomaticP scores >0.5, with lower stringency used to assess subclonal mutations in *Notch1*, *Trp53*, and *Pten*. Somatic variants within 20 Mb of the *Ptprc* gene (CD45.1) were removed. To visualize CNAs, we plotted calls larger than 20 Mb, and any smaller segments were merged with their largest neighbor.

Statistical analysis

Graphs and survival curves were plotted using GraphPad Prism with Log-rank Mantel-Cox test used to compare survival significance.

Online supplementary material

Fig. S1 shows phenotypic evolution, TCR-β expression, and cell cycle analyses of developmentally arrested thymocytes in *Lmo2*-transgenic mice. Fig. S2 shows kinetic studies detailing the emergence of transplantable, clonal thymocyte populations in *Lmo2*-transgenic mice. Fig. S3 shows thymocyte analyses and competitive BM transplantation studies demonstrating that *BCL2* overexpression restores T cell development and competitive fitness of T cell progenitors in *Lmo2*-transgenic mice. Fig. S4 shows cell cycle, TCR-β expression, thymocyte transplantation, and *Notch1* mutation analyses, demonstrating that pre-LSCs do not develop in *Lmo2*;*BCL2* double transgenic mice. Fig. S5 shows a model detailing the proposed role of impaired cell competition at the DN3 stage in the emergence of pre-LSCs in *Lmo2*-transgenic mice, as well as the inhibition of this process in the presence of BCL2 or WT lymphoid precursors. Table S1 shows a summary of the number of differentially expressed genes between *Lmo2*-transgenic and WT thymocyte populations. Tables S2, S3, and S4 show the differentially expressed genes between *Lmo2*-transgenic and WT young (2–3 wk old) DN2 thymocytes, young (2–3 wk old) DN3 thymocytes, and old (6–10 wk old) DN3 thymocytes, respectively.

Data availability

RNA-seq data are available in NCBI Gene Expression Omnibus (accession GSE188225) and exome sequencing data are available in NCBI Bioproject (accession PRJNA909315).

Acknowledgments

We thank Phillippe Bouillet (Walter and Eliza Hall Institute of Medical Research, Parkville, Australia), for *Vav-BCL2* transgenic mice, Adam Uldrich (Peter Doherty Institute for Infection and Immunity, Parkville, Australia) for technical assistance, and Samantha Ginn and Ian Alexander (Children's Medical Research Institute, Westmead, Australia) for discussions.

This work was supported by an Alan W. Harris Scholarship and an Australian Postgraduate Award (to H.D. Abdulla) from the Australian Government, project grants (1003391 to M.P. McCormack, 1187367 to D.H.D. Gray, and 1104145 to M.P. McCormack and I.J. Majewski), a Program grant (1113577 to W.S. Alexander), Fellowships (1154970 to G.K. Smyth, 1158024 to D.H.D. Gray, and 1058344 to W.S. Alexander), and the Independent Research Institute's Infrastructure Support Scheme from the National Health and Medical Research Council of Australia, a grant-in-aid from the Cancer Council of Victoria, a Future Fellowship from the Australian Research Council (to M.P. McCormack), and a Victorian State Government Operational Infrastructure Support grant.

Authorship contributions: H.D. Abdulla, R. Alserihi, W. Abeysekera, M.X. Luo, and C. Flensburg performed research; H.D. Abdulla, R. Alserihi, W. Abeysekera, M.X. Luo, and C. Flensburg analyzed data; X. Liu, D.H.D. Gray, G.K. Smyth, W.S. Alexander, I.J. Majewski, and M.P. McCormack supervised research; and H.D. Abdulla, C. Flensburg, X. Liu, D.H.D. Gray, G.K. Smyth, W.S. Alexander, I.J. Majewski, and M.P. McCormack wrote the paper.

Disclosures: The Walter and Eliza Hall Institute receives milestone and royalty payments related to Venetoclax, and employees may also be eligible for benefits related to these payments. W.S. Alexander and I.J. Majewski reported receiving payments from the Walter and Eliza Hall Institute related to Venetoclax. M.P. McCormack is an employee of iCamuno Biotherapeutics and has served as a consultant for AstraZeneca. D.H.D. Gray reported "other" from Walter and Eliza Hall Institute and grants from Servier outside the submitted work. X. Liu is co-founder of iCamuno Biotherapeutics. No other disclosures were reported.

Submitted: 26 November 2021
Revised: 19 December 2022
Accepted: 22 February 2023

References

Abdulla, H., A. Vo, B.J. Shields, T.J. Davies, J.T. Jackson, R. Alserihi, E.M. Viney, T. Wong, F. Yan, N.C. Wong, et al. 2021. T-ALL can evolve to oncogene independence. *Leukemia*. 35:2205–2219. https://doi.org/10.1038/s41375-021-01120-9

Abraham, B.J., D. Hnisz, A.S. Weintraub, N. Kwiatkowski, C.H. Li, Z. Li, N. Weichert-Leahey, S. Rahman, Y. Liu, J. Etchin, et al. 2017. Small genomic insertions form enhancers that misregulate oncogenes. *Nat. Commun.* 8:14385. https://doi.org/10.1038/ncomms14385

Belver, L., and A. Ferrando. 2016. The genetics and mechanisms of T cell acute lymphoblastic leukaemia. *Nat. Rev. Cancer*. 16:494–507. https://doi.org/10.1038/nrc.2016.63

Belyaev, N.N., J. Biró, D. Athanasakis, D. Fernandez-Reyes, and A.J. Potocnik. 2012. Global transcriptional analysis of primitive thymocytes reveals accelerated dynamics of T cell specification in fetal stages. *Immunogenetics*. 64:591–604. https://doi.org/10.1007/s00251-012-0620-6

Boehm, T. 2012. Self-renewal of thymocytes in the absence of competitive precursor replenishment. *J. Exp. Med.* 209:1397–1400. https://doi.org/10.1084/jem.20121412

Braun, C.J., K. Boztug, A. Paruzynski, M. Witzel, A. Schwarzer, M. Rothe, U. Modlich, R. Beier, G. Göhring, D. Steinemann, et al. 2014. Gene therapy for Wiskott-Aldrich syndrome--long-term efficacy and genotoxicity. *Sci. Transl. Med.* 6:227ra33. https://doi.org/10.1126/scitranslmed.3007280

Chambers, J., and T.H. Rabbitts. 2015. LMO2 at 25 years: A paradigm of chromosomal translocation proteins. *Open Biol.* 5:150062. https://doi.org/10.1098/rsob.150062

Chen, S., S. Nagel, B. Schneider, M. Kaufmann, C. Meyer, M. Zaborski, U.R. Kees, H.G. Drexler, and R.A. MacLeod. 2011. Novel non-TCR chromosome translocations t(3;11)(q25;p13) and t(X;11)(q25;p13) activating LMO2 by juxtaposition with MBNL1 and STAG2. *Leukemia*. 25:1632–1635. https://doi.org/10.1038/leu.2011.119

Chiang, M.Y., L. Xu, O. Shestova, G. Histen, S. L'heureux, C. Romany, M.E. Childs, P.A. Gimotty, J.C. Aster, and W.S. Pear. 2008. Leukemia-associated NOTCH1 alleles are weak tumor initiators but accelerate K-ras-initiated leukemia. *J. Clin. Invest.* 118:3181–3194. https://doi.org/10.1172/JCI35090

Cleveland, S.M., S. Smith, R. Tripathi, E.M. Mathias, C. Goodings, N. Elliott, D. Peng, W. El-Rifai, D. Yi, X. Chen, et al. 2013. Lmo2 induces hematopoietic stem cell-like features in T-cell progenitor cells prior to leukemia. *Stem Cells*. 31:882–894. https://doi.org/10.1002/stem.1345

Curtis, D.J., and M.P. McCormack. 2010. The molecular basis of Lmo2-induced T-cell acute lymphoblastic leukemia. *Clin. Cancer Res.* 16:5618–5623. https://doi.org/10.1158/1078-0432.CCR-10-0440

Dik, W.A., B. Nadel, G.K. Przybylski, V. Asnafi, P. Grabarczyk, J.M. Navarro, B. Verhaaf, C.A. Schmidt, E.A. Macintyre, J.J. van Dongen, and A.W. Langerak. 2007. Different chromosomal breakpoints impact the level of LMO2 expression in T-ALL. *Blood*. 110:388–392. https://doi.org/10.1182/blood-2006-12-064816

Egle, A., A.W. Harris, M.L. Bath, L. O'Reilly, and S. Cory. 2004. VavP-Bcl2 transgenic mice develop follicular lymphoma preceded by germinal center hyperplasia. *Blood*. 103:2276–2283. https://doi.org/10.1182/blood-2003-07-2469

Eguchi-Ishimae, M., M. Eguchi, H. Kempski, and M. Greaves. 2008. NOTCH1 mutation can be an early, prenatal genetic event in T-ALL. *Blood*. 111:376–378. https://doi.org/10.1182/blood-2007-02-074690

Ferrando, A.A., D.S. Neuberg, J. Staunton, M.L. Loh, C. Huard, S.C. Raimondi, F.G. Behm, C.H. Pui, J.R. Downing, D.G. Gilliland, et al. 2002. Gene expression signatures define novel oncogenic pathways in T cell acute lymphoblastic leukemia. *Cancer Cell*. 1:75–87. https://doi.org/10.1016/S1535-6108(02)00018-1

Flensburg, C., T. Sargeant, A. Oshlack, and I.J. Majewski. 2020. SuperFreq: Integrated mutation detection and clonal tracking in cancer. *PLOS Comput. Biol.* 16:e1007603. https://doi.org/10.1371/journal.pcbi.1007603

Gao, J., M. Van Meter, S. Hernandez Lopez, G. Chen, Y. Huang, S. Ren, Q. Zhao, J. Rojas, C. Gurer, G. Thurston, and F. Kuhnert. 2019. Therapeutic targeting of Notch signaling and immune checkpoint blockade in a spontaneous, genetically heterogeneous mouse model of T-cell acute lymphoblastic leukemia. *Dis. Model. Mech.* 12:12. https://doi.org/10.1242/dmm.040931

García-Ramírez, I., S. Bhatia, G. Rodríguez-Hernández, I. González-Herrero, C. Walter, S. González de Tena-Dávila, S. Parvin, O. Haas, W. Woessmann, M. Stanulla, et al. 2018. Lmo2 expression defines tumor cell identity during T-cell leukemogenesis. *EMBO J.* 37:e98783. https://doi.org/10.15252/embj.201798783

Gerby, B., C.S. Tremblay, M. Tremblay, S. Rojas-Sutterlin, S. Herblot, J. Hébert, G. Sauvageau, S. Lemieux, E. Lécuyer, D.F. Veiga, et al. 2014. SCL, LMO1 and Notch1 reprogram thymocytes into self-renewing cells. *PLoS Genet.* 10:e1004768. https://doi.org/10.1371/journal.pgen.1004768

Ginn, S.L., C.V. Hallwirth, S.H.Y. Liao, E.T. Teber, J.W. Arthur, J. Wu, H.C. Lee, S.S. Tay, M. Hu, R.R. Reddel, et al. 2017. Limiting thymic precursor supply increases the risk of lymphoid malignancy in murine X-linked severe combined immunodeficiency. *Mol. Ther. Nucleic Acids*. 6:1–14. https://doi.org/10.1016/j.omtn.2016.11.011

Ginn, S.L., S.H. Liao, A.P. Dane, M. Hu, J. Hyman, J.W. Finnie, M. Zheng, M. Cavazzana-Calvo, S.I. Alexander, A.J. Thrasher, et al. 2010. Lymphomagenesis in SCID-X1 mice following lentivirus-mediated phenotype correction independent of insertional mutagenesis and gammac overexpression. *Mol. Ther.* 18:965–976. https://doi.org/10.1038/mt.2010.50

Ginn, S.L., M.P. McCormack, and I.E. Alexander. 2018. Thymocyte self-renewal and oncogenic risk in immunodeficient mouse models: Relevance for human gene therapy clinical trials targeting haematopoietic stem cell populations?. *Mamm. Genome*. 29:771–776. https://doi.org/10.1007/s00335-018-9780-5

Girardi, T., C. Vicente, J. Cools, and K. De Keersmaecker. 2017. The genetics and molecular biology of T-ALL. *Blood*. 129:1113–1123. https://doi.org/10.1182/blood-2016-10-706465

Goossens, S., and P. Van Vlierberghe. 2017. Novel oncogenic noncoding mutations in T-ALL. *Blood*. 129:3140–3142. https://doi.org/10.1182/blood-2017-04-773242

Göthert, J.R., R.L. Brake, M. Smeets, U. Dührsen, C.G. Begley, and D.J. Izon. 2007. NOTCH1 pathway activation is an early hallmark of SCL T leukemogenesis. *Blood*. 110:3753–3762. https://doi.org/10.1182/blood-2006-12-063644

Hacein-Bey-Abina, S., A. Garrigue, G.P. Wang, J. Soulier, A. Lim, E. Morillon, E. Clappier, L. Caccavelli, E. Delabesse, K. Beldjord, et al. 2008. Insertional oncogenesis in 4 patients after retrovirus-mediated gene therapy of SCID-X1. *J. Clin. Invest.* 118:3132–3142. https://doi.org/10.1172/JCI35700

Hacein-Bey-Abina, S., C. Von Kalle, M. Schmidt, M.P. McCormack, N. Wulffraat, P. Leboulch, A. Lim, C.S. Osborne, R. Pawliuk, E. Morillon, et al. 2003. LMO2-associated clonal T cell proliferation in two patients after gene therapy for SCID-X1. *Science*. 302:415–419. https://doi.org/10.1126/science.1088547

Herblot, S., A.M. Steff, P. Hugo, P.D. Aplan, and T. Hoang. 2000. SCL and LMO1 alter thymocyte differentiation: Inhibition of E2A-HEB function and pre-T alpha chain expression. *Nat. Immunol.* 1:138–144. https://doi.org/10.1038/77819

Hnisz, D., A.S. Weintraub, D.S. Day, A.L. Valton, R.O. Bak, C.H. Li, J. Goldmann, B.R. Lajoie, Z.P. Fan, A.A. Sigova, et al. 2016. Activation of proto-oncogenes by disruption of chromosome neighborhoods. *Science*. 351:1454–1458. https://doi.org/10.1126/science.aad9024

Howe, S.J., M.R. Mansour, K. Schwarzwaelder, C. Bartholomae, M. Hubank, H. Kempski, M.H. Brugman, K. Pike-Overzet, S.J. Chatters, D. de Ridder, et al. 2008. Insertional mutagenesis combined with acquired somatic mutations causes leukemogenesis following gene therapy of SCID-X1 patients. *J. Clin. Invest.* 118:3143–3150. https://doi.org/10.1172/JCI35798

Iacobucci, I., and C.G. Mullighan. 2017. Genetic basis of acute lymphoblastic leukemia. *J. Clin. Oncol.* 35:975–983. https://doi.org/10.1200/JCO.2016.70.7836

Koboldt, D.C., Q. Zhang, D.E. Larson, D. Shen, M.D. McLellan, L. Lin, C.A. Miller, E.R. Mardis, L. Ding, and R.K. Wilson. 2012. VarScan 2: Somatic mutation and copy number alteration discovery in cancer by exome sequencing. *Genome Res.* 22:568–576. https://doi.org/10.1101/gr.129684.111

Koch, U., and F. Radtke. 2011. Notch in T-ALL: New players in a complex disease. *Trends Immunol.* 32:434–442. https://doi.org/10.1016/j.it.2011.06.005

Larson, R.C., P. Fisch, T.A. Larson, I. Lavenir, T. Langford, G. King, and T.H. Rabbitts. 1994. T cell tumours of disparate phenotype in mice transgenic for Rbtn-2. *Oncogene*. 9:3675–3681.

Larson, R.C., H. Osada, T.A. Larson, I. Lavenir, and T.H. Rabbitts. 1995. The oncogenic LIM protein Rbtn2 causes thymic developmental aberrations that precede malignancy in transgenic mice. *Oncogene*. 11:853–862.

Law, C.W., Y. Chen, W. Shi, and G.K. Smyth. 2014. voom: Precision weights unlock linear model analysis tools for RNA-seq read counts. *Genome Biol.* 15:R29. https://doi.org/10.1186/gb-2014-15-2-r29

Li, H., and R. Durbin. 2009. Fast and accurate short read alignment with Burrows-Wheeler transform. *Bioinformatics*. 25:1754–1760. https://doi.org/10.1093/bioinformatics/btp324

Liao, Y., G.K. Smyth, and W. Shi. 2019. The R package Rsubread is easier, faster, cheaper and better for alignment and quantification of RNA sequencing reads. *Nucleic Acids Res.* 47:e47. https://doi.org/10.1093/nar/gkz114

Lin, Y.W., R.A. Nichols, J.J. Letterio, and P.D. Aplan. 2006. Notch1 mutations are important for leukemic transformation in murine models of precursor-T leukemia/lymphoma. *Blood*. 107:2540–2543. https://doi.org/10.1182/blood-2005-07-3013

Liu, Y., J. Easton, Y. Shao, J. Maciaszek, Z. Wang, M.R. Wilkinson, K. McCastlain, M. Edmonson, S.B. Pounds, L. Shi, et al. 2017. The genomic landscape of pediatric and young adult T-lineage acute lymphoblastic leukemia. *Nat. Genet.* 49:1211–1218. https://doi.org/10.1038/ng.3909

Mansour, M.R., V. Duke, L. Foroni, B. Patel, C.G. Allen, P.J. Ancliff, R.E. Gale, and D.C. Linch. 2007. Notch-1 mutations are secondary events in some patients with T-cell acute lymphoblastic leukemia. *Clin. Cancer Res.* 13:6964–6969. https://doi.org/10.1158/1078-0432.CCR-07-1474

Martins, V.C., K. Busch, D. Juraeva, C. Blum, C. Ludwig, V. Rasche, F. Lasitschka, S.E. Mastitsky, B. Brors, T. Hielscher, et al. 2014. Cell competition is a tumour suppressor mechanism in the thymus. *Nature*. 509:465–470. https://doi.org/10.1038/nature13317

Martins, V.C., E. Ruggiero, S.M. Schlenner, V. Madan, M. Schmidt, P.J. Fink, C. von Kalle, and H.R. Rodewald. 2012. Thymus-autonomous T cell development in the absence of progenitor import. *J. Exp. Med.* 209:1409–1417. https://doi.org/10.1084/jem.20120846

Matthews, J.M., K. Lester, S. Joseph, and D.J. Curtis. 2013. LIM-domain-only proteins in cancer. *Nat. Rev. Cancer*. 13:111–122. https://doi.org/10.1038/nrc3418

McCarthy, D.J., and G.K. Smyth. 2009. Testing significance relative to a fold-change threshold is a TREAT. *Bioinformatics*. 25:765–771. https://doi.org/10.1093/bioinformatics/btp053

McCormack, M.P., and D.J. Curtis. 2010. The thymus under siege: Lmo2 induces precancerous stem cells in a mouse model of T-ALL. *Cell Cycle*. 9:2267–2268. https://doi.org/10.4161/cc.9.12.12074

McCormack, M.P., and T.H. Rabbitts. 2004. Activation of the T-cell oncogene LMO2 after gene therapy for X-linked severe combined immunodeficiency. *N. Engl. J. Med.* 350:913–922. https://doi.org/10.1056/NEJMra032207

McCormack, M.P., L.F. Young, S. Vasudevan, C.A. de Graaf, R. Codrington, T.H. Rabbitts, S.M. Jane, and D.J. Curtis. 2010. The Lmo2 oncogene initiates leukemia in mice by inducing thymocyte self-renewal. *Science*. 327:879–883. https://doi.org/10.1126/science.1182378

Michalak, E.M., C.J. Vandenberg, A.R. Delbridge, L. Wu, C.L. Scott, J.M. Adams, and A. Strasser. 2010. Apoptosis-promoted tumorigenesis: Gamma-irradiation-induced thymic lymphomagenesis requires puma-driven leukocyte death. *Genes Dev.* 24:1608–1613. https://doi.org/10.1101/gad.1940110

Ogilvy, S., D. Metcalf, C.G. Print, M.L. Bath, A.W. Harris, and J.M. Adams. 1999. Constitutive Bcl-2 expression throughout the hematopoietic compartment affects multiple lineages and enhances progenitor cell survival. *Proc. Natl. Acad. Sci. USA*. 96:14943–14948. https://doi.org/10.1073/pnas.96.26.14943

Paiva, R.A., A.G.G. Sousa, C.V. Ramos, M. Ávila, J. Lilue, T. Paixão, and V.C. Martins. 2021. Self-renewal of double-negative 3 early thymocytes enables thymus autonomy but compromises the β-selection checkpoint. *Cell Rep.* 35:108967. https://doi.org/10.1016/j.celrep.2021.108967

Peaudecerf, L., G. Krenn, P. Gonçalves, F. Vasseur, and B. Rocha. 2016. Thymocytes self-renewal: A major hope or a major threat?. *Immunol. Rev.* 271:173–184. https://doi.org/10.1111/imr.12408

Peaudecerf, L., S. Lemos, A. Galgano, G. Krenn, F. Vasseur, J.P. Di Santo, S. Ezine, and B. Rocha. 2012. Thymocytes may persist and differentiate without any input from bone marrow progenitors. *J. Exp. Med.* 209:1401–1408. https://doi.org/10.1084/jem.20120845

Qasim, W., H.B. Gaspar, and A.J. Thrasher. 2014. "Darwinian" tumor-suppression model unsupported in clinical experience. *Mol. Ther.* 22:1562–1563. https://doi.org/10.1038/mt.2014.147

Rahman, S., M. Magnussen, T.E. León, N. Farah, Z. Li, B.J. Abraham, K.Z. Alapi, R.J. Mitchell, T. Naughton, A.K. Fielding, et al. 2017. Activation of the LMO2 oncogene through a somatically acquired neomorphic promoter in T-cell acute lymphoblastic leukemia. *Blood*. 129:3221–3226. https://doi.org/10.1182/blood-2016-09-742148

Ramos, C.V., L. Ballesteros-Arias, J.G. Silva, R.A. Paiva, M.F. Nogueira, J. Carneiro, E. Gjini, and V.C. Martins. 2020. Cell competition, the kinetics of thymopoiesis, and thymus cellularity are regulated by double-negative 2 to 3 early thymocytes. *Cell Rep.* 32:107910. https://doi.org/10.1016/j.celrep.2020.107910

Ritchie, M.E., B. Phipson, D. Wu, Y. Hu, C.W. Law, W. Shi, and G.K. Smyth. 2015. Limma powers differential expression analyses for RNA-sequencing and microarray studies. *Nucleic Acids Res.* 43:e47. https://doi.org/10.1093/nar/gkv007

Robinson, M.D., D.J. McCarthy, and G.K. Smyth. 2010. edgeR: a Bioconductor package for differential expression analysis of digital gene expression data. *Bioinformatics*. 26:139–140. https://doi.org/10.1093/bioinformatics/btp616

Robinson, M.D., and A. Oshlack. 2010. A scaling normalization method for differential expression analysis of RNA-seq data. *Genome Biol.* 11:R25. https://doi.org/10.1186/gb-2010-11-3-r25

Roels, J., M. Thénoz, B. Szarzyńska, M. Landfors, S. De Coninck, L. Demoen, L. Provez, A. Kuchmiy, S. Strubbe, L. Reunes, et al. 2020. Aging of pre-leukemic thymocytes drives CpG island hypermethylation in T-cell

acute lymphoblastic leukemia. *Blood Cancer Discov.* 1:274–289. https://doi.org/10.1158/2643-3230.BCD-20-0059

Ruggero, K., O. Al-Assar, J.S. Chambers, R. Codrington, T. Brend, and T.H. Rabbitts. 2016. LMO2 and IL2RG synergize in thymocytes to mimic the evolution of SCID-X1 gene therapy-associated T-cell leukaemia. *Leukemia*. 30:1959–1962. https://doi.org/10.1038/leu.2016.116

Schiroli, G., S. Ferrari, A. Conway, A. Jacob, V. Capo, L. Albano, T. Plati, M.C. Castiello, F. Sanvito, A.R. Gennery, et al. 2017. Preclinical modeling highlights the therapeutic potential of hematopoietic stem cell gene editing for correction of SCID-X1. *Sci. Transl. Med.* 9:9. https://doi.org/10.1126/scitranslmed.aan0820

Shank-Calvo, J.A., K. Draheim, M. Bhasin, and M.A. Kelliher. 2006. p16Ink4a or p19Arf loss contributes to Tal1-induced leukemogenesis in mice. *Oncogene*. 25:3023–3031. https://doi.org/10.1038/sj.onc.1209326

Shields, B.J., C.I. Slape, N. Vo, J.T. Jackson, A. Pliego-Zamora, H. Ranasinghe, W. Shi, D.J. Curtis, and M.P. McCormack. 2019. The NUP98-HOXD13 fusion oncogene induces thymocyte self-renewal via Lmo2/Lyl1. *Leukemia*. 33:1868–1880. https://doi.org/10.1038/s41375-018-0361-0

Sincennes, M.C., M. Humbert, B. Grondin, V. Lisi, D.F. Veiga, A. Haman, C. Cazaux, N. Mashtalir, B. Affar, A. Verreault, and T. Hoang. 2016. The LMO2 oncogene regulates DNA replication in hematopoietic cells. *Proc. Natl. Acad. Sci. USA*. 113:1393–1398. https://doi.org/10.1073/pnas.1515071113

Smith, S., R. Tripathi, C. Goodings, S. Cleveland, E. Mathias, J.A. Hardaway, N. Elliott, Y. Yi, X. Chen, J. Downing, et al. 2014. LIM domain only-2 (LMO2) induces T-cell leukemia by two distinct pathways. *PLoS One*. 9:e85883. https://doi.org/10.1371/journal.pone.0085883

Tatarek, J., K. Cullion, T. Ashworth, R. Gerstein, J.C. Aster, and M.A. Kelliher. 2011. Notch1 inhibition targets the leukemia-initiating cells in a Tal1/Lmo2 mouse model of T-ALL. *Blood*. 118:1579–1590. https://doi.org/10.1182/blood-2010-08-300343

Treanor, L.M., E.J. Volanakis, S. Zhou, T. Lu, C.J. Sherr, and B.P. Sorrentino. 2011. Functional interactions between Lmo2, the Arf tumor suppressor, and Notch1 in murine T-cell malignancies. *Blood*. 117:5453–5462. https://doi.org/10.1182/blood-2010-09-309831

Tremblay, C.S., F.C. Brown, M. Collett, J. Saw, S.K. Chiu, S.E. Sonderegger, S.E. Lucas, R. Alserihi, N. Chau, M.L. Toribio, et al. 2016. Loss-of-function mutations of Dynamin 2 promote T-ALL by enhancing IL-7 signalling. *Leukemia*. 30:1993–2001. https://doi.org/10.1038/leu.2016.100

Tremblay, M., C.S. Tremblay, S. Herblot, P.D. Aplan, J. Hébert, C. Perreault, and T. Hoang. 2010. Modeling T-cell acute lymphoblastic leukemia induced by the SCL and LMO1 oncogenes. *Genes Dev.* 24:1093–1105. https://doi.org/10.1101/gad.1897910

Van Vlierberghe, P., M. van Grotel, H.B. Beverloo, C. Lee, T. Helgason, J. Buijs-Gladdines, M. Passier, E.R. van Wering, A.J. Veerman, W.A. Kamps, et al. 2006. The cryptic chromosomal deletion del(11)(p12p13) as a new activation mechanism of LMO2 in pediatric T-cell acute lymphoblastic leukemia. *Blood*. 108:3520–3529. https://doi.org/10.1182/blood-2006-04-019927

Wu, D., and G.K. Smyth. 2012. Camera: A competitive gene set test accounting for inter-gene correlation. *Nucleic Acids Res.* 40:e133. https://doi.org/10.1093/nar/gks461

Wu, L., Y. Xu, Q. Wang, C. Ruan, H.G. Drexler, D. Wu, R.A. MacLeod, and S. Chen. 2015. High frequency of cryptic chromosomal rearrangements involving the LMO2 gene in T-cell acute lymphoblastic leukemia. *Haematologica*. 100:e233–e236. https://doi.org/10.3324/haematol.2014.120089

Zhou, S., S. Fatima, Z. Ma, Y.D. Wang, T. Lu, L.J. Janke, Y. Du, and B.P. Sorrentino. 2016. Evaluating the safety of retroviral vectors based on insertional oncogene activation and blocked differentiation in cultured thymocytes. *Mol. Ther.* 24:1090–1099. https://doi.org/10.1038/mt.2016.55

Supplemental material

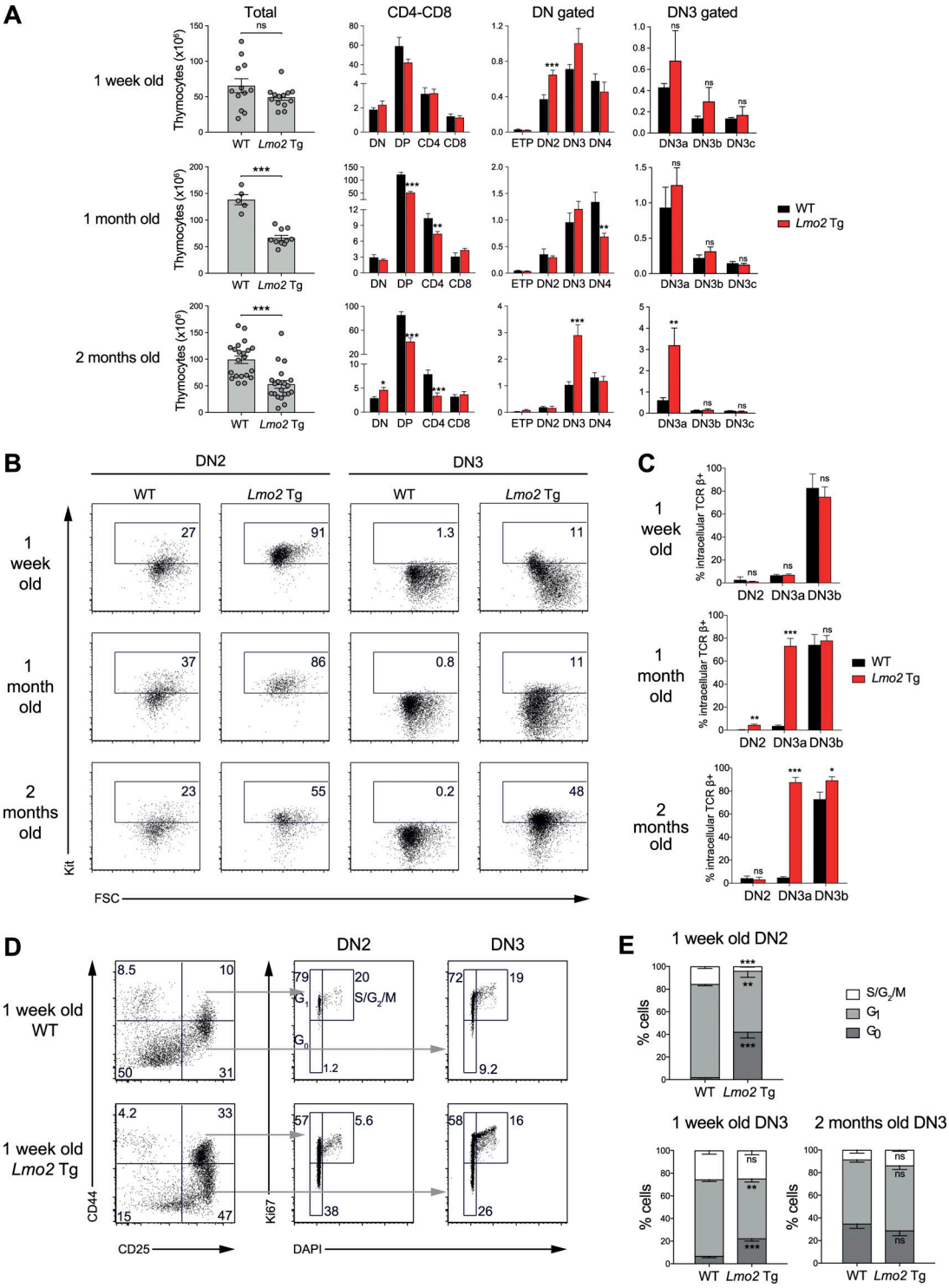

Figure S1. **Phenotypic evolution, TCR-β expression, and cell cycle analysis of developmentally arrested thymocytes in *Lmo2*-transgenic mice. (A)** Numbers of total thymocytes (left column) and individual thymocyte subsets, in *Lmo2*-transgenic mice at the indicated ages. DN3 thymocytes were sub-fractionated into DN3a-c subsets using CD28 vs. CD25 staining by flow cytometry. For total thymocytes, points show individual mice and lines show mean ± SEM. Data are from 5–14 separate experiments. **(B)** Time course of Kit expression in DN2 and DN3 thymocytes in *Lmo2*-transgenic (Tg) mice. Representative flow cytometric analysis of Kit expression in DN2 and DN3 thymocytes from WT and *Lmo2*-transgenic mice of the indicated ages. Numbers indicate the percentage of Kit⁺ cells. FSC, forward scatter. Data are representative of three to six separate experiments. **(C)** Self-renewing *Lmo2*-transgenic DN3a thymocytes contain intracellular TCR-β. FACS analysis was used to identify the percentage of intracellular TCR-β in DN2, DN3a, and DN3b thymocytes from WT and *Lmo2*-transgenic mice of the indicated ages. Data are mean + SEM of *n* = 3–8 per group. **(D and E)** Developmentally arrested DN2 thymocytes in young *Lmo2*-transgenic are quiescent. **(D)** Cell cycle analysis of DN2 and DN3 thymocytes from 1-wk-old WT and *Lmo2*-transgenic mice, showing the percentage of cells in G_0, G_1, and $S/G_2/M$ phases. **(E)** Percentage of DN2 and DN3 thymocytes in each cell cycle phase as in D. Results are mean – SEM (1 wk old, *n* = 4–5 mice per group; 2 mo old, *n* = 4 mice per group from three to four separate experiments). *P < 0.05, **P < 0.01, and ***P < 0.001 (Student's *t* test).

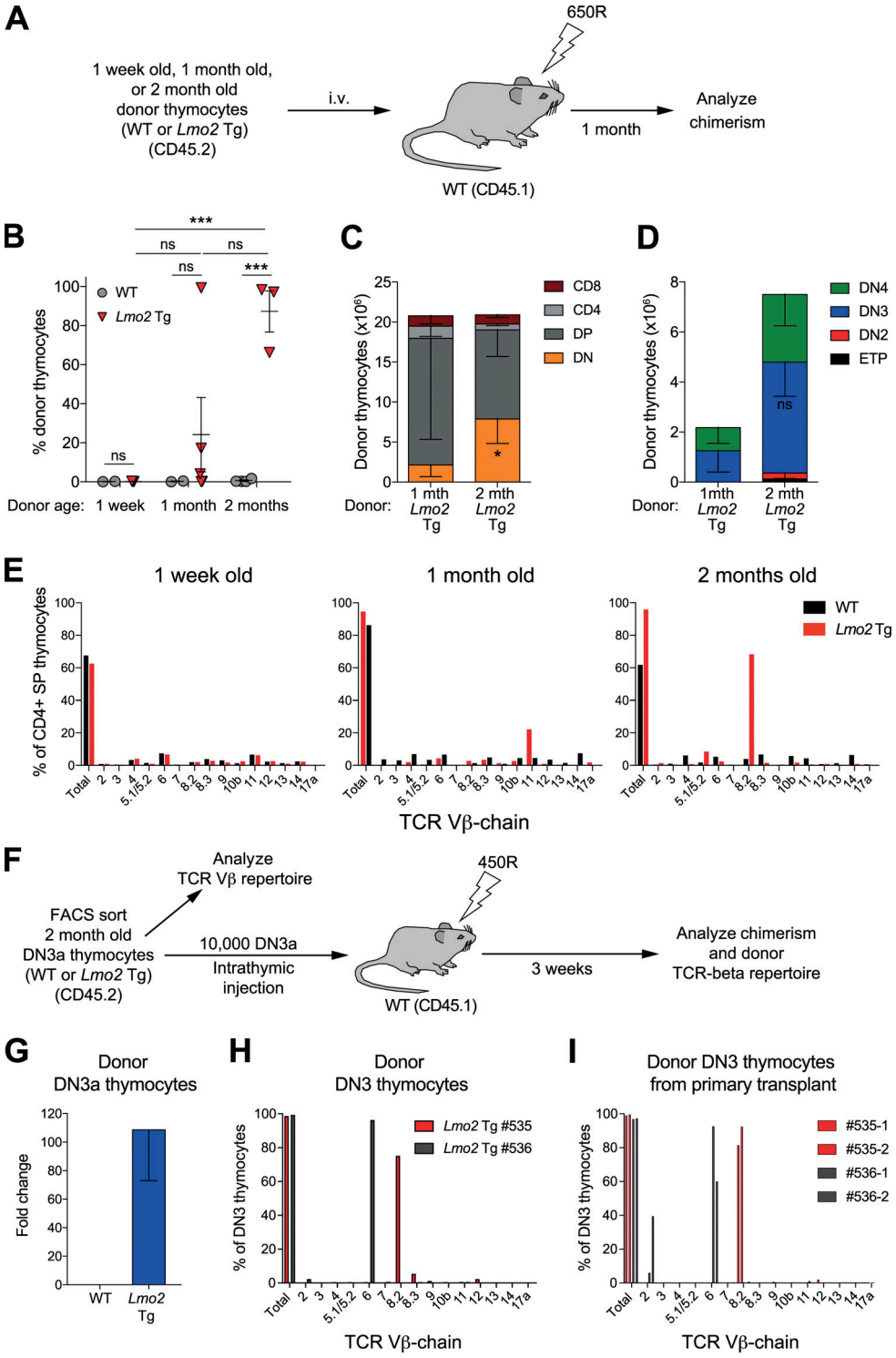

Figure S2. **Transplantable, clonal thymocyte populations arise by 2 mo of age in *Lmo2*-transgenic mice. (A)** Schematic of experimental strategy to determine the long-term engraftment capacity of *Lmo2*-transgenic (Tg) thymocytes. **(B)** Percentage of donor thymocytes in the thymi of mice transplanted with WT or *Lmo2*-transgenic thymocytes of the indicated ages at 1 mo after transplant. Points show the average chimerism of 1–3 recipients from each donor mouse and lines show mean ± SEM. Data are from two to four separate experiments. ***P < 0.001 (Student's *t* test). **(C and D)** Total numbers of total (C) and DN (D) donor thymocytes in the thymi of mice receiving *Lmo2*-transgenic donor cells of the indicated ages, as in B, at 1 mo after transplant. Results are mean – SEM of 6–10 mice from two to three separate experiments. *P < 0.05 (Student's *t* test). **(E)** Analysis of TCR Vβ subfamily usage in CD4$^+$ SP thymocytes from WT and *Lmo2*-transgenic mice of the indicated ages. Bars denote data from individual mice. Data are representative of two to six mice from two to five separate experiments. **(F)** Experimental strategy to examine clonal composition of transplantable Lmo2-transgenic thymocytes. **(G)** Fold change in the number donor DN3a thymocytes in recipient thymi at 3 wk after transplant (relative to the number of transplanted cells). Results show the mean – SEM of *n* = 2 (WT) and *n* = 5 (*Lmo2*-transgenic) from one to two experiments. **(H and I)** TCR Vβ subfamily usage in donor DN3 thymocytes at the time of transplantation (H) and 3 wk after transplantation (I). Colors represent recipients transplanted with DN3a thymocytes from individual donor mice.

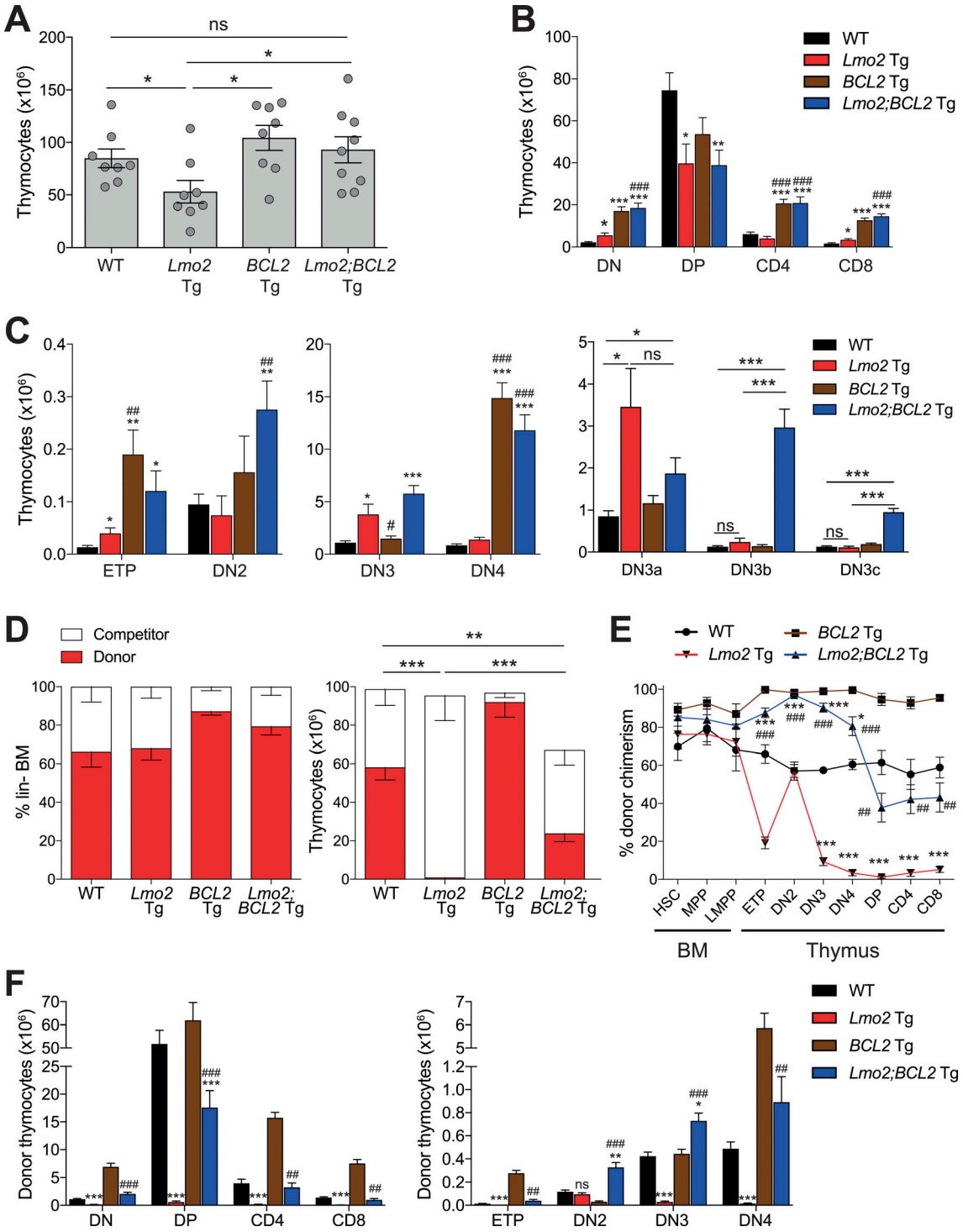

Figure S3. ***BCL2* overexpression restores T cell development and competitive fitness of T cell progenitors in *Lmo2*-transgenic mice. (A–C)** Analysis of T cell subsets in the thymi. Numbers of total thymocytes (A) and different thymocyte subsets (B and C) in mice of the indicated genotypes at 6–8 wk of age were determined by flow cytometry. In A, points represent individual mice and lines show mean ± SEM. In B and C, data are mean ± SEM of eight to nine mice per group from six experiments. *P < 0.05, **P < 0.01, and ***P < 0.001 vs. WT, ##P < 0.01, ###P < 0.001 vs. *Lmo2* transgenic (Tg; Student's *t* test). **(D–F)** Competitive BM transplantation using *Lmo2;BCL2* double transgenic cells. Competitive BM transplantation experiments were performed as in Fig. 2 A. **(D)** Analysis of donor/competitor contribution of BM and thymus at 4 wk after transplant. The percentage of donor/competitor BM (left panel) and total number of donor/competitor thymocytes (right panel) are shown. **(E)** Contribution of donor BM of the indicated genotypes to progenitor populations in the BM (HSC, multipotent progenitor [MPP], and LMPP) and stages of T cell development in the thymus (ETP, DN2, DN3, DN4, DP, CD8, and CD8) at 4 wk after transplant. **(F)** Absolute numbers of donor T cell subsets at 4 wk post-transplant. Results are mean ± SEM. *P < 0.05, **P < 0.01, ***P < 0.001 compared to WT, ##P < 0.01, ###P < 0.001 compared to *Lmo2*-transgenic (Student's *t* test). WT (n = 5), *Lmo2*-transgenic (n = 9), BCL2 transgenic (n = 5), and *Lmo2;BCL2* double transgenic (n = 12) from three independent experiments.

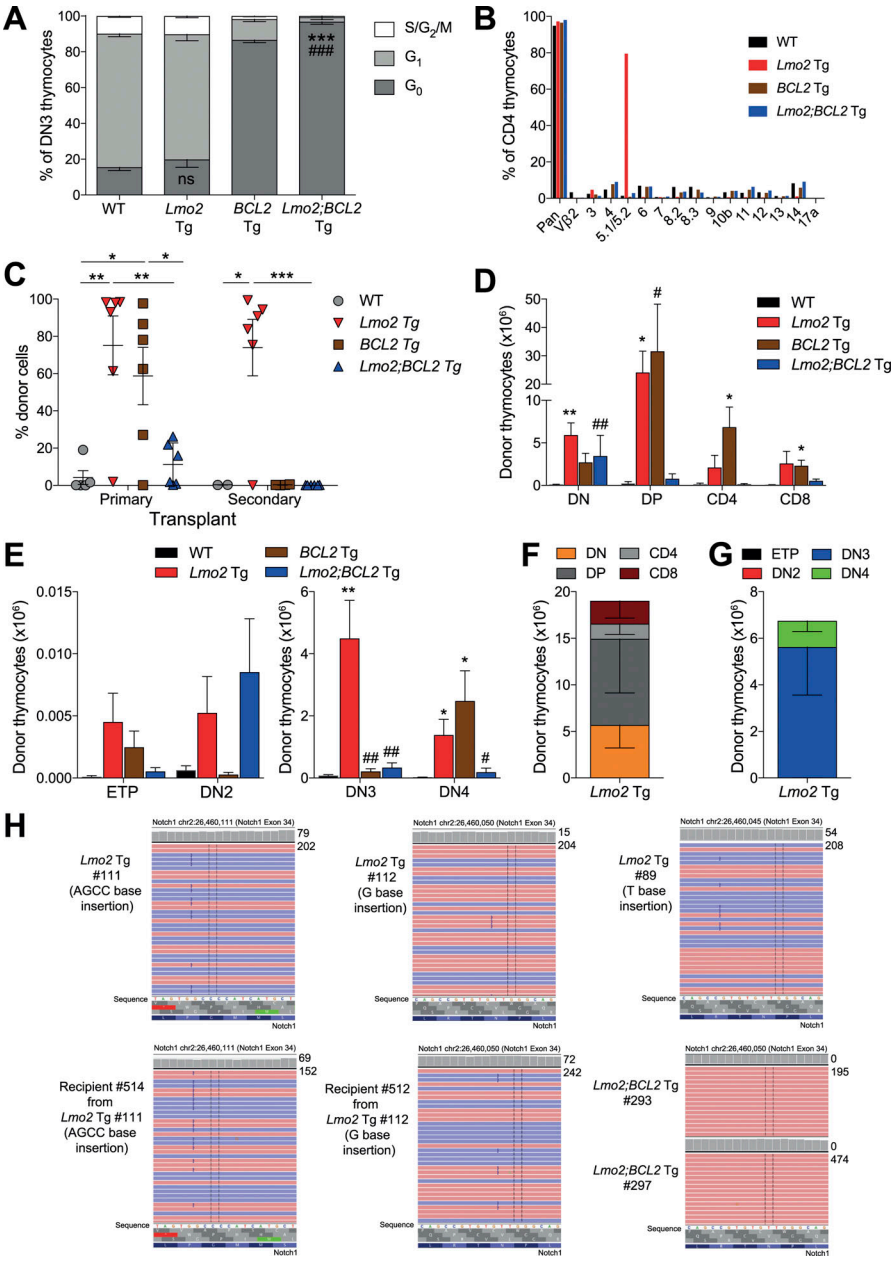

Figure S4. **Pre-LSCs do not develop in *Lmo2;BCL2* double transgenic mice. (A)** Cell cycle analysis of DN3 thymocytes from 2-mo-old WT, *Lmo2*, *BCL2*, and *Lmo2;BCL2* transgenic (Tg) mice, showing the percentage of cells in G_0, G_1, and $S/G_2/M$ phases. Cell cycle analysis was performed as in Fig. S1 D. Results are mean – SEM of *n* = 5–6 per group from five experiments. ***P < 0.001 compared to WT, ###P < 0.001 compared to *Lmo2*-transgenic (Student's *t* test). **(B)** TCR Vβ subfamily usage in $CD4^+$ SP thymocytes of mice of the indicated genotypes. Note the presence of a dominant clone in *Lmo2*-transgenic thymocytes that is absent in *Lmo2;BCL2* double transgenic thymocytes. Bars denote data from individual mice. Data are representative of 4–6 mice per group from four separate experiments. **(C–F)** *Lmo2;BCL2* double transgenic thymocytes lack serial engraftment capacity. Sublethally irradiated (650 rad) CD45.1 WT mice were injected with thymocytes equivalent to one-quarter of a thymus from 2-mo-old WT, *Lmo2*, *BCL2*, and *Lmo2;BCL2* transgenic mice (all CD45.2). 1 mo after transplant, recipient thymi were harvested and donor/recipient cell contribution was determined by flow cytometry. Thymocytes equivalent to one-quarter of a thymus were then used for secondary transplantations. **(C)** Percentage of donor thymocytes from primary and secondary recipient thymi at 1 mo after transplant. Points show the average chimerism of one to three recipients from each donor mouse and lines show mean ± SEM. Data are from four experiments (primary) and one to four experiments (secondary transplants). *P < 0.05, **P < 0.01, and ***P < 0.001 vs. WT (Student's *t* test). **(D and E)** Number of total (D) and DN (E) donor thymocytes in thymi of primary transplant recipient mice as in C. Results are mean + SEM. *P < 0.05, **P < 0.01 compared to WT, #P <0.05, ##P <0.01 compared to *Lmo2*-transgenic (Student's *t* test). **(F and G)** Number of total (F) and DN (G) donor thymocytes in thymi of secondary transplant recipient mice as in C. Results are mean – SEM of six recipients. **(H)** Analysis of Notch1 mutations in preleukemic thymocytes of *Lmo2*-transgenic and *Lmo2;BCL2* double transgenic mice. RNA-seq track of 2-mo-old *Lmo2*-transgenic DN3a thymocytes (#89, #111, and #112) and recipient mice #514, and #512 DN3a thymocytes (which were transplanted with *Lmo2*-transgenic #111, and #112 DN3a thymocytes, respectively) showing reads mapped to exon 34 of Notch1. Insertion mutations found are indicated in parentheses. Numbers on upper right corner of images indicate the number of reads with insertions (top) and total read count (bottom). RNA-seq track of 2-mo-old *Lmo2;BCL2* double transgenic DN3a thymocytes (lower right) showing reads mapped to exon 34 of *Notch1*, displaying a lack of *Notch1* mutations.

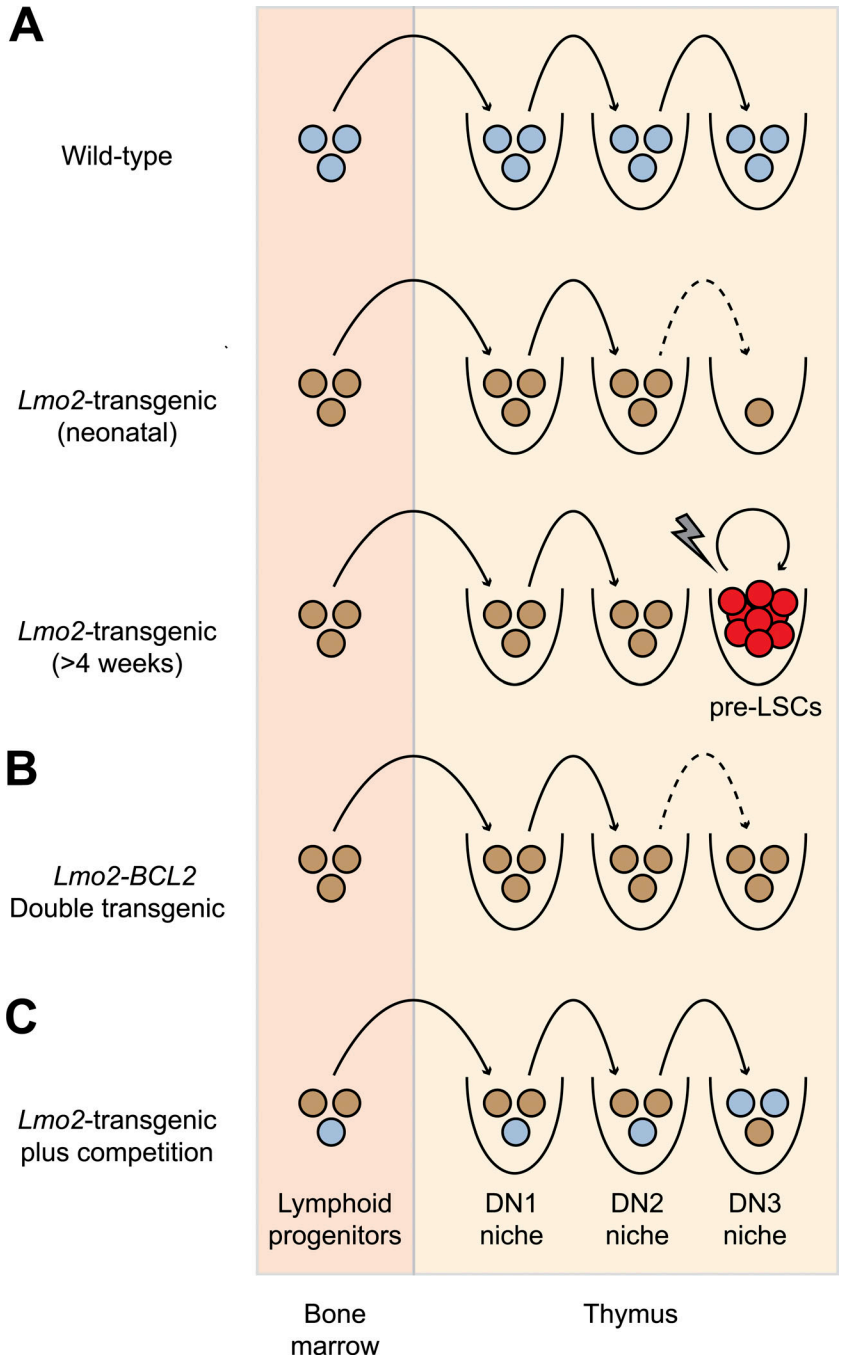

Figure S5. **Model of LMO2-induced T-ALL leukemogenesis. (A)** Lymphoid progenitors from the BM seed the thymus, where they encounter niches supporting various stages of T cell development (DN1–3). *Lmo2*-transgenic cells (brown) have a defect at the DN2–DN3 transition (dashed arrow) relative to WT progenitors (blue). This causes a decrease in "new" DN3 thymocytes in neonatal mice, with small numbers of residual DN3 thymocytes residing in a vacated niche, resulting in increased proliferation. By 4–8 wk of age, *Lmo2*-transgenic DN3 thymocytes acquire mutations in the *Notch1* PEST domain (lightning bolt), resulting in the development of self-renewing pre-LSCs (red, with self-renewal indicated by circular arrow) that are the origin of T-ALL in this model. Note that continued expression of LMO2 is required for continued survival and self-renewal of pre-LSCs (Abdulla et al., 2021). **(B)** In the presence of *BCL2* transgene, the loss of *Lmo2*-transgenic DN3 thymocytes does not occur. This leads to filling of the DN3 niche, which prevents the proliferative stress on DN3 thymocytes and thereby prevents secondary mutations such as *Notch1* mutations that result in the development of pre-LSCs. **(C)** Similarly, the presence of WT competitor cells (blue) in competitive BM transplantation experiments restores cellular competition at the DN3 stage. This also inhibits proliferation of *Lmo2*-transgenic DN3 thymocytes (brown) and thereby prevents the acquisition of secondary mutations that cause the development of pre-LSCs.

Provided online are four tables. Table S1 shows a summary of the number of differentially expressed genes between *Lmo2*-transgenic and WT thymocyte populations used in this study. Table S2 shows the differentially expressed genes between *Lmo2*-transgenic and WT young (2–3 wk old) DN2 thymocytes. Table S3 shows the differentially expressed genes between *Lmo2*-transgenic WT young (2–3 wk old) DN3 thymocytes. Table S4 shows the differentially expressed genes between *Lmo2*-transgenic and WT old (6–10 wk old) DN3 thymocytes.